

**IOSUD – „DUNĂREA DE JOS” UNIVERSITY OF GALAȚI**  
**The School for Doctoral Studies in Engineering**



# **DOCTORAL THESIS**

## **ABSTRACT**

# **CONTRIBUTIONS CONCERNING THE INFLUENCE OF THE NAVAL STRUCTURE’S GEOMETRY ON THE STRESSES UNDER IMPACT LOADS**

**Doctorand,**  
**Manuela NECHITA**

**Conducător științific,**  
**Prof. univ. dr. ing. Costel Iulian MOCANU**

**Seria I6 Inginerie mecanică Nr. 50**

**GALAȚI**  
**2020**



**IOSUD - „DUNĂREA DE JOS” UNIVERSITY OF GALAȚI**  
**The School for Doctoral Studies in Engineering**



# **DOCTORAL THESIS**

## **ABSTRACT**

**CONTRIBUTIONS CONCERNING THE INFLUENCE OF NAVAL STRUCTURE'S GEOMETRY ON  
STRESSES UNDER IMPACT LOADS**

**Doctorand,**

**Manuela NECHITA**

**Conducător științific,**

Prof univ.dr.ing. **Costel Iulian MOCANU**

**Referenți științifici**

Prof univ.dr.ing. **DHC Anton HADĂR**

Prof univ.dr.ing. **Ioan-Călin ROȘCA**

Prof univ.dr. ing. **Leonard DOMNIȘORU.**

**Seria I6 Inginerie mecanică Nr. 50**

**GALAȚI**

**2020**



***If you want to build a ship, do not start by sending people for wood, nails, tools, twine and other materials. Instead, teach them to yearn for the vast and endless sea.***

*Antoine de Saint Exupery*



NS Mircea in parade (80 years), Galati, 19 September 2019



# FOREWORD

River navigation currently holds a significant share of all freight transport, in central Europe this being one third of the total traffic. In 2011, on the Danube River included in the Pan-European Corridor VII, Romania accounted for 58.4% of the total goods transport on navigable channels. The unfavorable weather conditions can disrupt these activities, by naval accidents that can cause the damaged barges structure due collision.

Depending on the transported goods, which may be lost in the navigable channels, it can lead to environmental pollution. Even if there is a low risk coefficient for inland waterway accidents, the shipwreck may block the waterway, with great negative economic effects.

Without knowing the answer due to the real stress types encountered in the use under real operating conditions, the attempt to improve a naval structure can lead to its premature surrender.

In order to design a naval structure with a high impact resistance, this paper presents a comparative study of the impact behaviour of naval structure's geometry.

## **The purpose and objectives of the work:**

The main purpose of this paper is to design a procedure for checking and modifying the geometry of the barge 's bow structure, which responds to the safety assurance requirements in operation, in case of accident. The 2000T barge was chosen for this study, which is most often used for freight transport on inland waters, respectively on the Danube-Rhine canals system.

## **General objectives:**

Experimental and numerical analyses development methodologies for assessing the influence of geometry on the stresses and the damages, that occurs as a result of the mechanical impact phenomena on the metallic naval structures.

## **Specific objectives:**

1. Analysis of the general aspects regarding the response of the naval structures under impact loads.
2. Development of an experimental methodology for determining the elasto-plastic deformations at impact between bodies.
3. Comparative study, using the Finite Element Method, for various impact scenarios, at different speeds, of the stricken barge's components behavior under impact loads.
4. The comparative study for different types of structures obtained from the initial one by modifying the thicknesses of the constructive elements of the shipboard as well as by modifying its curvature
5. Establishing solutions to adequately modify the structure of the barge (ships in general), to minimize the collision effects between floating structures.
6. Assessment of design solutions to reduce the damage of a naval structure under impact loads.

This work consists of six chapters divided as follows:

**Chapter 1** The current state of research on the impact of naval structures.

**Chapter 2** Research methodology of the impact phenomenon on metallic structures.

**Chapter 3** Preliminary study of a naval structure under impact loads.

**Chapter 4** Study of the influence of geometry on the stresses of naval structure under impact loads.

**Chapter 5** Study of the geometry's influence on a struck naval structure's rupture.

**Chapter 6** Final conclusions, original contributions and future research perspectives.

The theme of this thesis is highly topical research, the knowledge in this field is still at the beginning in Romania and therefore other methods of solving and experimental tests can be approached than those presented here.

# TABLE OF CONTENTS

		Pp. abstract	Pp. thesis
	Acknowledgements.....	I	I
	Keywords.....		II
	Foreword.....	I	III
Chapter 1.	The current state of research on the impact of naval structures .....	3	3
	1.1. External dynamics of naval structure under impact loads.....	3	3
	1.2. Internal dynamics of naval structure under impact loads.....	4	4
	1.2.1. Methods for analysing structural damage.....	4	4
	1.2.2. The basis of external energy transformation in dissipation energy .....	5	8
	1.3. Experimental analysis of naval structures under impact loads .....	6	13
	1.3.1. Laboratory tests.....	7	15
	1.3.2. Full-scale experiment.....	8	20
	1.4. Numerical simulation of naval structures under impact loads.....	8	21
	1.5. Concluding remarks .....	9	24
Chapter 2.	Research methodology of the impact phenomenon on metallic structures .....	11	27
	2.1. Research methodology.....	11	27
	2.1.1. Test stand and equipment used for experimental study of the impact on a curved plate .....	11	27
	2.1.2. Experimental analysis of the impact on curved plates .....	12	28
	2.1.3. Numerical analysis of the impact on curved plates .....	13	30
	2.2. Data analysis on the influence of geometry on the stress and deformation.....	18	37
	2.3. Concluding remarks .....	19	38
Chapter 3.	Preliminary study of a naval structure under impact loads .....	21	39
	3.1. Preliminary study of a naval structure for structural analysis.....	21	39
	3.1.1. Geometric modeling of a naval structure (CAD Method)	21	39
	3.1.2. Structural modeling of a naval structure's geometry (Finite Element Method).....	22	41
	3.2. Structural analysis of a naval structure under impact loads (Finite Element Method).....	23	43
	3.3. Data post-processing.....	24	44
	3.4. Concluding remarks.....	25	50
Chapter 4.	Study of the influence of geometry on the stresses of naval structure under impact loads .....	27	51
	4.1. Study on a naval structure under side impact loads.....	27	51



	Pp. abstract	Pp. thesis
4.1.1 The impact's selection procedure for a naval structure ....	27	51
4.1.2. A model structural analysis under impact loads .....	27	52
4.1.3. Data analysis.....	29	56
4.2. Study of the influence of geometry on the stresses under impact loads .....	30	60
4.3. Variants of diminishing Von Mises stress under impact loads ..	32	63
4.3.1. Studying the influence of friction on the side impact of naval structures with redesigned geometry .....	32	64
4.3.2. Studying the influence of the redesigned geometry on the stresses under impact loads .....	33	66
4.4. Concluding remarks .....	34	67
Chapter 5. Study of the geometry's influence on a struck naval structure's rupture.....	35	69
5.1. Impact scenarios on the starboard of a naval structure .....	35	69
5.1.1. Evaluation of the effects due to the impact loads with 100 kJ.....	35	71
5.1.2. Evaluation of the effects due to the impact loads with 100 kJ.....	38	75
5.1.3 The analysis of the unmodified structure geometry's influence on the effects due to the impact depending on the friction coefficients between the elements of the structure and the impactor.....	40	80
5.1.4. Study of the effects due to the impact loads at tensile tearing failure mode.....	42	84
5.2. Design solutions to reduce collision effects .....	44	92
5.2.1. Redesign of the structure' s geometric characteristics (the shell's and frame 's element thickness's modification).....	44	92
5.2.2. Redesign the curvature of the frame .....	47	99
5.2.3 Evaluation the influence of frame's curvature on the effects due to the impact loads.....	50	108
5.3. Concluding remarks.....	53	114
Chapter 6. Final conclusions. Personal contributions. Future research perspectives.....	55	117
6.1. Final conclusions.....	55	117
6.2. Personal contributions .....	57	120
6.3. Future research perspectives.....	58	121
List of published and presented papers.....		123
Bibliography.....	61	125

### **Scientific Supervisor,**

Prof. dr.ing. Costel Iulian Mocanu

### **Guidance Commission**

Prof. dr.ing. Iulian Gabriel Bîrsan

Prof. dr.ing. Leonard Domnişoru

Conf. dr.ing. Gabriel Popescu

## CHAPTER 1

## THE CURRENT STATE OF RESEARCH ON THE IMPACT OF NAVAL STRUCTURES

**The objectives are pursued:**

1. the study of the external-internal dynamics of the impacted naval structures;
2. studying the experimental analysis of the impacted naval structures;
3. studying the numerical simulation of the impacted naval structures.

The main research directions of the impact phenomenon in the naval field will be highlighted.

**1.1. External dynamics of naval structure under impact loads**

The ship is considered a rigid body with 6 degrees of freedom (Fig. 1.1, Table 1.1):

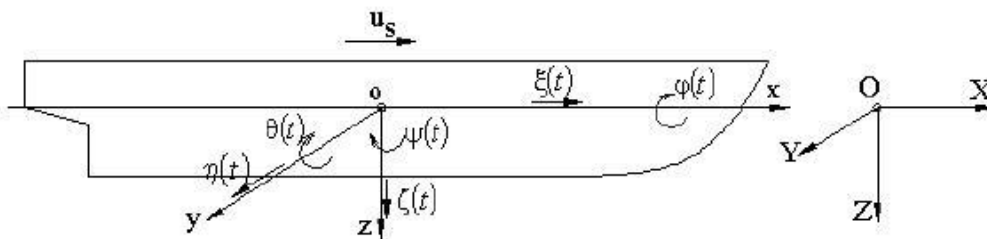


**Fig.1.** The degrees of freedom at the oscillation of the rigid body ship, coordinate systems [1]

**Table 1.1** Ship's degrees of freedom

displacement	rotation
surge $\xi(t)$ 1	roll $\varphi(t)$ 4
sway $\eta(t)$ 2	pitch $\theta(t)$ 5
heave $\zeta(t)$ 3	yaw $\psi(t)$ 6

The determination of the impulses due to the impact and the energy of collision dissipated in the damage of the ship are performed by an analytical procedure, and the analysis is restricted to the movement of the ship in the plane from the surface of the water.

In 1982, Petersen [2] presented a procedure in which the external dynamics of naval collisions were simulated in time. The hydrodynamics of the forces acting on the body of the ship during the collision were calculated using the strip theory. The ships involved were considered as rigid bodies with deformations only in the contact area. The responses of the structures in the contact area were modeled as non-linear springs. Also Woisin [3] performed an external analysis of a ship-to-ship collision and estimated kinetic energy losses. In this case the collision was considered to be completely plastic. A similar analysis procedure was developed by Pawlowski [4] and Hanhirona [5]. Also in these works the ships were considered to be completely rough, without allowing any slide in the contact area.

Zhang [6] developed an analytical method that describes energy loss and impact momentum for an arbitrary ship-to-ship collision. At the beginning of the calculation he considered that the ship has displacements in the direction of the X axis (surge motion) and displacements in the direction of the Y axis (sway motion), and had analyzed the sliding and rebounding, in the plane of the surface of the water, during the collision. The energy lost by dissipation in the structural deformations of the structures involved is expressed by closed-form

expressions. The procedure is based on the rigid body mechanics, where the strain energy due to impact loads outside the contact region is negligible. Because the contact region is considered small and local this allows Zhang [6] to assume the collision instantaneously as each body exerts an impulsive force on the other at the point of contact. The model includes the friction between the impact surfaces that are identified as the glancing blows situations.

Numerical examples of ship-to-ship collision at different points and angles of impact are comparable to the results obtained by time-field simulations. This shows that the procedure which is based on rigid body mechanics is sufficiently accurate for the analysis of ship-to-ship collision [6].

Zhang considers for collision study that the striking ship (ship A) sails at speeds  $v_{ax}$  and  $v_{ay}$  and collided the struck ship (ship B), sailing at speeds  $v_{b1}$ ,  $v_{b2}$ .

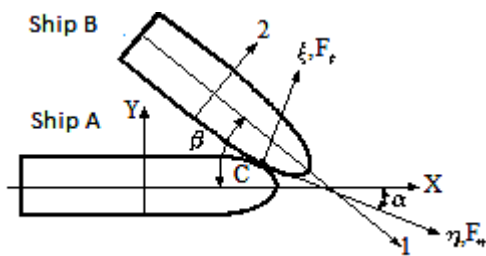


**Fig.1.2** The coordinate system used at the collision of ships [6]

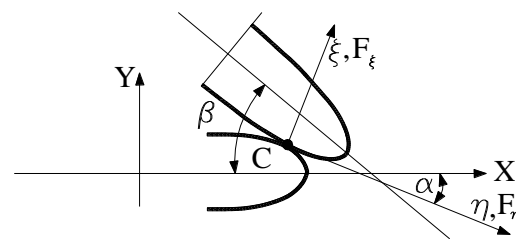


**Fig.1.3** The coordinate system  $\xi \eta$  used at the collision of ships (detail)

An XYZ-coordinate system is considered fixed to the sea bottom. The Z- axis is chosen in out of the water direction, the X- axis lies in the symmetry plane of the striking vessel pointed towards the bow and the origin of the XYZ- system is placed so that the midship section is in the YZ plane at the moment.  $t=0$ , as in Fig.1.2. In Fig.1.3 is presented the origin of the system is located at point C of impact, the axis  $\xi$  is normal to the impact surface, the angle between the X axis and  $\eta$  is  $\alpha$ , and the angle between axis X and axis 1 is  $\beta$ .

## 1.2. Internal dynamics of naval structure under impact loads

### 1.2.1. Methods for analysing structural damage

The internal dynamics studies the way in which the deformation energy is dissipated in the striking and struck objects and involves the evaluation of the structural resistance during the large deformations, by using the theory of plasticity or the finite element method. Thus, the structural response during the collision is analysed and simplified calculation methods are established for the force-penetration curve, the relationship between the absorbed energy and the penetration and the resulting damage in the ship structures. The ship is considered to be a set of shell plating structures. Observations on existing models and collision's experiments show that the primary energy absorbing mechanism of the board structures are [6]:

- membrane deformation of the boards and attached stiffeners
- folding and crushing of transverse frames and longitudinal stringers
- folding, cutting and crushing horizontal decks
- cutting or crushing the bottom of the ship
- crushing of bulkheads

The existing methods for analysing the structural damages in ship collisions are divided into four categories:

1. Empirical methods
2. Finite element method
3. Experimental methods
4. Simplified methods

In this paragraph only the first and last method are presented, in the following paragraphs the other two categories are described.

The most well-known empirical method was introduced by Minorsky [7] who analysed 26 collision cases and developed a formula for determining the material destroyed during ship collisions.

The empirical formula proposed by Minorsky [7] indicates that the energy absorbed by a ship during the collision is directly proportional to the volume of material destroyed. Therefore, if a ship is designed to withstand collisions, it is oversized. It is not entirely true, as long as the energy absorption efficiency differs from one structure to another. It depends on the arrangement of the structure, the material properties and the manner of destruction.

Thus Zhang [6] established a relationship between the absorbed energy and the destroyed volume, which considers the arrangement of structures, material properties and size of damage. The method was validated by experiments and numerical simulations. The method is an alternative to the Minorsky method. The proposed formulas take into account the following three energy absorption mechanisms:

1. energy absorption by the plastic tension damage mode;
2. energy absorption by the crushing and folding damage mode;
3. energy absorption by the tearing damage mode.

Reckling [10] proposed a method that took into account the deformation of both the striking ship and the struck ship. The energy absorbed in both ships, until the body of the struck ship was broken, was calculated by simple methods. An example calculation was made for two oil tankers of 141,000 tdw. The results showed that the energy absorbed under membrane tension of the board is only 18% of the total energy, while the energy absorbed in the web frames, decks and the bottom of the struck ship is 40% of the total energy. The bow structure of the ship that generated the collision absorbed 42% of the total energy. Pedersen et al. [11] studied the loads that led to the crushing of the bow of the ships. In the analysis, the formulas proposed by Gerard [12], Amdahl [13], and Yang and Caldwell [14] were applied. Similarly, Pedersen [15] obtained an empirical expression for side collision, which can be used in collision with supporting elements of the bridges.

### 1.2.2. The basis of external energy transformation in dissipation energy

A simplified method (or limit analysis), widely used in engineering analysis and design, is used. It has been shown that the method is valid for estimating the limit load of a structure subjected to extreme loads. The limit load thus obtained can be used as a real design basis. Limit analysis method is an approximate method.

In the limit analysis method, a key point is the construction of the kinematically admissible speed and the displacement field. It is based on observations obtained during existing experimental tests, accidents or analysis studies. It is well known that the yield stress for mild steel is very sensitive to the strain rate. Jones [22] has shown experimentally that the yield stress for a mild steel increases with the increase of strain rate.

If a structure is deformed enough, it will rupture and cause damage. Predicting fracture of a structure is a very complicated problem. Different loads cause different failure modes.

Jones et.al. [6], [23] discussed the rupture criteria of the ductile metal beams subjected to large dynamic loads.

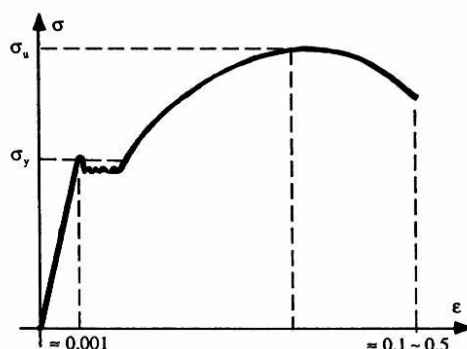


**Fig.1.6** Typical stress-strain diagram

As Simonsen [21] noted, simplified methods are based on overall deformation mechanisms. The maximum strain failure criterion has been used in many researches by some well-known authors such as Wang [24] and Paik and Pedersen [20]. According to this criterion when the strain of the structure reaches maximum critical strain value, the structure ruptures.

In practical calculations, the specific critical strain of the material for the prediction of structural failure must be known.

In general, this results from axial tensile experiments. An usual stress-strain curve specific for a mild steel is shown in Fig.1.6

The experiments carried out by Wen and Jones [25] and Amdahl [26] showed that the tensile ductility of a mild steel is between 0.20 and 0.35. Amdahl [27] emphasized that due to the scale effect and material imperfections, this value is too large for the assessment of naval collisions. The critical strain value suggested by Amdahl [27] for side collisions is between 5% and 10%. In the minor collisions analyzed by McDermott et.al. [28], the critical rupture strain for the mild steel materials in case of side collisions was evaluated from:

$$\varepsilon_c = 0.10 \left( \frac{\varepsilon_f}{0.32} \right) \quad (1.15)$$

where  $\varepsilon_f$  is tensile ductility. McDermott et.al. indicated that this formula was experimentally validated for the deformation of the shell plating.

When the critical rupture strain is known, the critical deflection or penetration of the shell plating can be determined.

### 1.3. Experimental analysis of naval structures under impact loads

Many experiments of ship collision were started in the early sixties of the 20th century. From 1962 to 1976 researchers in Italy, Germany and Japan performed a series of model tests. Some of the authors presented detailed results of these experiments, such as Amdahl [13], Jones [29], Ellina and Valsgard [30]. Samuelides [31], and Pedersen et.al. [11]. The main purpose of the experiments carried out in Italy, Germany and Japan was the ships designing to protect the nuclear reactor in case of collisions.

In Italy, 24 model experiments were performed to examine the efficiency of the structures of the different types of ship at impact with various types of striking ships [6].

Between 1967 and 1976, 12 ship models were tested in Germany [8]. The models were made on scales range from 1/12 to 1 / 7.5. The test procedure is shown in Fig. 1.8 illustrating the movement of the ship's striking bow along an inclined railway path. The ship's test shows

great damage as a result of the collision for the striking bow while the struck ship's that was designed with a special protective structure.

These experiments are difficult to perform because they require special financial and security conditions. In Fig.1.10, such an experiment is presented.

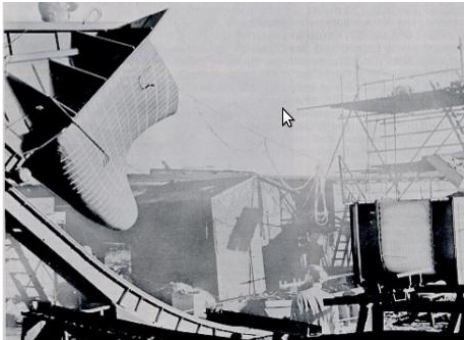


**Fig.1.8.** Experiments for ship collision in Germany [8]

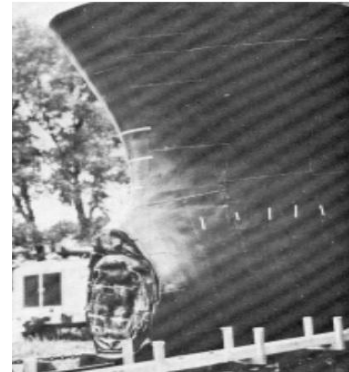


**Fig.1.10.** Destruction of bow after a collision test in Germany [6]

In this paragraph, a documentation regarding the experiments in the plastic field, realized on models both in the laboratory and in nature, is made.

### 1.3.1. Laboratory tests

Between 1966 and 1970 a series of model tests on collisions were performed in Japan. Both static and dynamic experiments were performed and covered different aspects of the specific problems of collisions such as, the design of the board's structure, the effect of the shape of the striking ship's test and the effect of the added mass. Details of the experiments were provided by Akita et.al. [31]. Amdahl and Kavlie [26] performed tests on models that simulated the body of the ship hit by a rigid hexagonal body. This original test simulated grounding, but it is also very useful in side collision analysis.



**Fig.1.13.** A 1:1 scale board model after a collision in Denmark [34]

Full-scale experiments were performed by Qvist et.al. [34], one being illustrated in Fig. 1.13.

In Japan, several tests have been carried out for the frontal collision of ships, such as Hagiwara et.al. [35] who used a 1/5 scale model for a 17,000 tdw freight with transverse frames. Wierzbicki [16] and Abramowicz and Jones [36] investigated the axial crushing of the basic structural elements [37] and Simonsen and Ocakli [34] from the Technical University of Denmark

conducted a series of model tests of web crushing.

### 1.3.2. Full-scale experiment

For 7 years (1991-1997), a project was developed in Japan that aimed to establish a methodology for predicting the behavior of the structure of an oil tank subject to impact. This project focused on two aspects. One was the dynamics of the process of damage of the structures due to the collision or grounding, and the other referred to the process of oil spill and / or the access of water through the body of the destroyed ship. A series of experiments were conducted in the Netherlands of Japan together with the Netherlands (1991). Two 80 m long oil tankers were used on an inland waterway. After the 1991 experiment, new experiments were carried out by Japan together with the Netherlands and Germany in November 1997. One 1500 t oil tanker collided with another 1500 t oil tank. The test area was chosen in the middle of the struck ship [6]. The experiment from 1998 is presented in Fig.1.23.



**Fig.1.23.** Collision experiment conducted in the Netherlands in 1998 [6]

### 1.4. Numerical simulation of naval structures under impact loads

The finite element method (FEM) is a powerful application of structural response analysis in collision study. There are several variants of software applications available such as LS-DYNA3D, ABAQUS, MSC / DYTRAN, FEMAP. Many researchers have used FEMs for collision analysis, such as Kitamura [39], Sano and Muragish [40] and Kuroiwa [41]. A typical example of FEM analysis for a collision made by Kitamura (1997) is shown in Fig. 1.24.

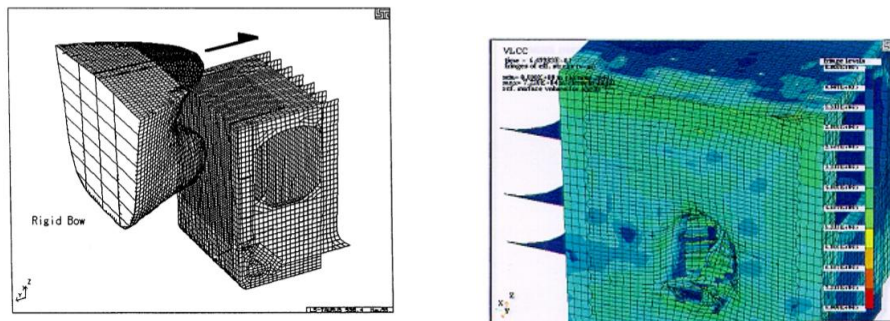


**Fig.1.24.** Simulation of ship-to-ship collision using FEM [39]

In the structural analysis Cook R.D. et. al. [42] consider that nonlinearity can be at least (sometimes all) geometric, material and / or boundary changing.

In solving nonlinear problems both methods are used to determine static and dynamic solutions. S.A.Myhre [43] and Cook R.D. et.al. [42] considers that the static solution method is used for finding the long-term response, for a structure subject to loads that vary slightly over time. However SAMyhre [43] recommends the dynamic solution method for the solutions in which the loads are dynamic or the duration of their application is small. Thus, the impact of a ship with an obstacle or another ship is studied with the last method because the interaction is short.

In finite element analysis, time cost is a dominant factor. The size of the time increment is limited by the smallest finite element. To complete the stability conditions the time increment must be less than the time required for the impact load to pass the element. If the time increment is too large, the request passes uncontrolled and causes an unstable structure.

For shell elements the critical size of the time increment is given by the formula:

$$\Delta t_c = \frac{L_s}{c} \quad (1.18)$$

where  $L_s$  is the characteristic length of an element and  $c$  is the speed of sound in the material given by the formula:

$$c = \sqrt{\frac{E}{\rho(1 - \nu^2)}} \quad (1.19)$$

where  $E$  is Young modulus,  $\rho$  is the density of the material and  $\nu$  is the Poisson coefficient.

## 1.5. Concluding remarks

Following the realized documentation, it was observed that the kinetic and potential energies appeared during the collision, analytically or experimentally, as well as the dissipated energies in the structure were determined in the studied literature. Because in the research naval field the experiments that study the impact phenomenon are very expensive, the obtained results are still references for numerical analyses carried out in the last years [46]. In these works the influence of the geometry of the struck naval structures on the response that appears in the hull due to the impact loads was not taken into account.

Thus, for this thesis, I chose to study the influence of the naval structures's geometry on the stresses under impact loads. I considered that the procedure proposed by Zhang [6] is accurate enough for collision analysis. The collision is symmetrical achieved at the water level, taking into account the frictional forces and neglecting the forces of inertia and the elastic energy appeared at impact [49].

The following two main objectives have been proposed for solving the theme and assessing the tensions due to the impact of the structure:

1. the diminish of the stress in the naval structure;
2. the diminish of the damaged area, as a result of the structure's collision.

In order to achieve these general objectives, the following specific objectives were obtained by derivation:



- analysis of the general aspects regarding the response of the naval structures under impact loads;
- experimental tests for the simulation of the impact of the curved metal plates;
- determining the displacements, as a response to the impact development of methodology for analyzing the impact phenomenon of curved plates;
- numerical analysis to identify the parameters that influence the impact phenomenon;
- analysis of the influence of the geometry of the naval structures on the stresses due to the impact loads;
- assessment of design solutions to reduce the damage of a naval structure under impact loads.

## CHAPTER 2

### RESEARCH METHODOLOGY OF THE IMPACT PHENOMENON ON METALLIC STRUCTURES

**The objectives of this chapter are as follows:**

1. experimental determination of the loads that appear in the metallic structure due to impact loads on a curved plate;
2. designing a methodology for numerical verification, by reconstructing the experiment performed on a curved plate;
3. analysis of the impact phenomenon the curved plates.

The purpose of this chapter is to elucidate the phenomenon of impact on curved plates in order to increase the internal energies at impact. The conclusions remark, after comparing the experimental analyses with the numerical simulations, allow choosing a suitable geometry at impact.

#### 2.1. Research methodology

In order to reach the objectives proposed for this research, the experiments were performed on the stand and on the equipment offered by the University Dunărea de Jos in Galați (UDJG), the experimental models being offered by the shipyard DAMEN S.A Galați. The experimental analysis was used as a starting point in the numerical investigations of the impact phenomenon on the metallic structures.

##### 2.1.1 Test stand and equipment used for experimental study of the impact on a curved plate

The experiments were performed in order to understand and then validate the numerical modeling at the impact of the metal structures.

The experimental stand used consists of: model steel plate curved rigidly mounted on rigid support made of steel, metal mass (sphere) known to achieve the impact and to determine the state of deformation, the Aramis HS GOM equipment, shown in Fig. 2.1. The experimental data provided by the GOM Aramis High Speed (HS) optical equipment, obtained after its calibration with a measurement accuracy of 0.04 pixels, were used [50] to determine the deformations due to the impact loads.



**Fig.2.1.** Aramis HS GOM equipment

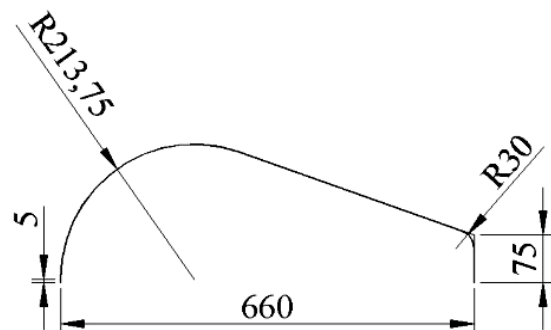


**Fig.2.2.** Cross section through model 1

The two model plates were made of naval steel, the first model ( $m_1 = 8.3003$  kg.) having the constructive shape shown in Fig.2.2, and area  $A_1 = 352455$  mm<sup>2</sup>. In order to obtain the shape of the curves specific to the model 2, the movement from point A (106.875, 185.11) to point B (106.875, 197.95) was performed. Curve 2 is mentioned in Fig.2.3. and it has the area  $A_2=356892$  mm<sup>2</sup> and the mass,  $m_2=8.4048$  kg.

Both models have the same thickness  $g = 3$  mm and the same size  $d = 300$  mm, in the direction of the Z axis, identifiable in Fig.2.3 and Fig.2.4. The behavior of the two model plates impacted with the steel mass of 5.37 kg was studied in the laboratory of strength materials within the university. The experimental system provides the results in the form of a database.

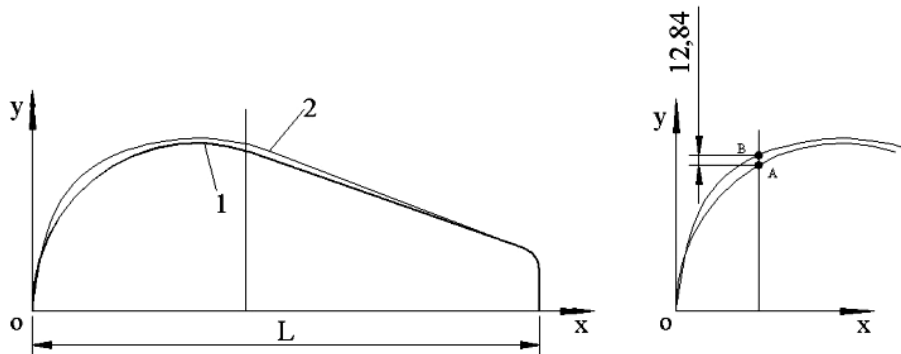


**Fig.2.3.** Cross section through model 2

### 2.1.2. Experimental analysis of the impact on curved plates

The body of the ship, from a constructive point of view, is a complex, elastic technical system, subject to the action of static and dynamic loads. The outer shell of the hull consists of straight and curved metal sheets of different sizes, stiffened frames and plates. The outer shell ensures both the tightness and resistance of the hull, together with the frame, to static and dynamic loads. Thus, in the naval design, the structural analysis of the outer shell of the hull is a field of research of real interest for the naval architects. The experiment conducted studies the behavior of two metal plates having different curves under impact loads.

Two experiments were performed for each model. The contact force of 1950 N was determined with an accelerator when the striking object collided with the models. The same ball launch height was maintained for all four experiments to control the impact energy. The wire with the length  $L = 300$ mm was considered inflexible and connected with the striking object.

In order to carry out measurements with the Aramis HS system, it was necessary to create a network of points on the surface of each model. In Fig.2.4 and Fig.2.5 is presented the model of painting its surface with white paint and sprinkling with black paint (both types of paint being matte).

This network allows measuring the displacements in time, by measuring the movement of these black dots in different intervals of time. The curved area, where the impact occurred, was filmed. The next table shows the displacements of the point with maximum deformations, during the 11 milliseconds of impact, the experiment for 6 seconds, followed in 800 steps. This is the maximum number of steps supported by the Aramis HS system. In this experiment, 17 analysis points were randomly selected from the database provided by the Aramis HS system.



**Fig. 2.4.** Preparing model experiment

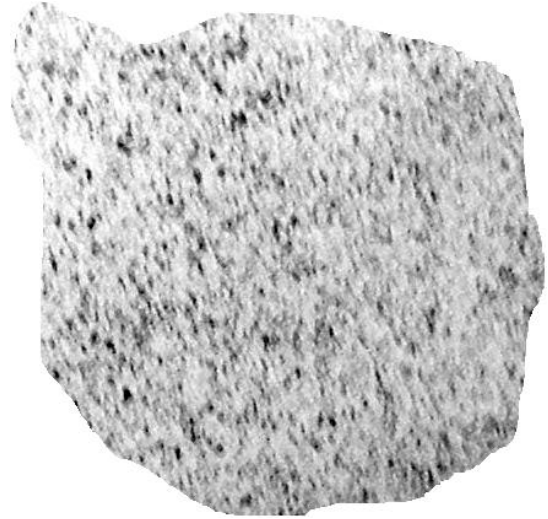


**Fig. 2.5.** Black dots network on the surface of the model painted in white

The experimental results are presented in Table 2.2.

**Table 2.2.** Maximum displacement of the studied points for the two impacted models

Model	Maximum displacement (mm)	Studied point
1	5.01	7
2	4.22	7

2.1.3. Numerical analysis of the impact on curved plates

The numerical simulation, performed with finite elements in FEMAP application 11.4, allowed the non-linear modeling of the plates, as in Fig. 2.7. The non-linear modeling of the plate material was chosen to study the behavior in the elastoplastic field.

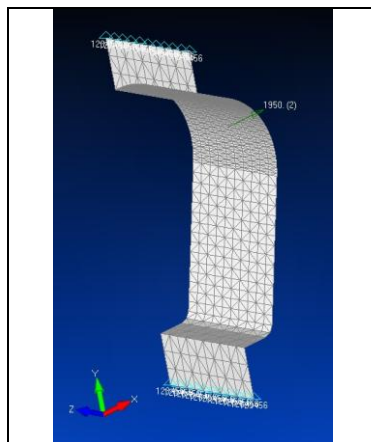


**Fig.2.7.** Finite element modelling of the model plate 1 and the striking object

Both static and dynamic non-linear modelings were performed to study the variation of deformations and stresses as well as the deformation energy due to the impact loads. In these simulations the impact or object was considered rigid and for the plate a behavior defined in FEMAP was chosen using bilinear elastoplastic material, with the option of isotropic hardening. The components of the impact force,  $F = 1950 \text{ N}$ , are considered distributed only in the X and Y axes direction, on the Z direction its component being null. The angle of the impacting force relative to the X axis has the value  $\alpha_1 = 27^\circ$  for model 1, respectively  $\alpha_2 = 28^\circ$  for model 2.

**Table 2.3.** Simulation data plate model - striking object

Nr.crt	Analysis type	Mesh		Boundary conditions
		Model 1	Model 2	
Model plate	static and dynamic	1960 shell elements	1960 shell elements	Fixed on 2 sides as in Fig. 2.1
striking object	dynamic	1573 shell elements	1660 shell elements	-

The ADINA solver was used to solve the dynamic impact problem and the obtained database was interpreted in the same application. The design data regarding the characteristics of the two materials used for simulation are included in Table 2.3 and Table 2.4.

**Table 2.4.** S235 steels non-linear properties

Object	Elastic modulus E (Pa)	Poisson coefficient	Density (Kg/m <sup>3</sup> )	Tangent modulus (Pa)	Yield stress (Pa)
Striking object	2.1E11	0.30	7850	-	-
Model plate	2.1E11	0.30	7850	0.1E06	235E06

Static modeling was used to verify the numerical modeling of the material and used, for integration, the full Newton Raphson method, as an option of the Nastran- Femap application. Subsequently, the material chosen, the impact dynamic modeling is carried out. The area of interest is illustrated in Fig. 2.8.

The maximum values of the deformations in the nodes, respectively the Von Mises stresses on the elements of the two models in the case of static modeling, are shown in the diagrams of Fig.2.9, Fig.2.10, Fig.2.11 and Fig.2.12. For the contact nodes, the coordinates, expressed in meters, are considered: nod 523 - model 1 ( $x=0.212$ ,  $y=0.301$ ,  $z=0.15$ ) and nod 497- model 2 ( $x=0.217$ ,  $y=0.301$ ,  $z=0.150$ ).

For dynamic modeling, the impact force was defined using a time function, for duration of 11 milliseconds, similar to the impact phenomenon from the experimental analysis. Due to the short time, the explicit direct integration method, with the explicit Nonlinear Advance option, is used to find the solution. In the diagrams in Fig.2.14, Fig.2.15, Fig.2.16 and Fig.2.17, the results of the analysis are presented, the maximum values being similar, as a type, with those mentioned in the static analysis

a) Static numerical simulation of the impact in the application FEMAP 11.4

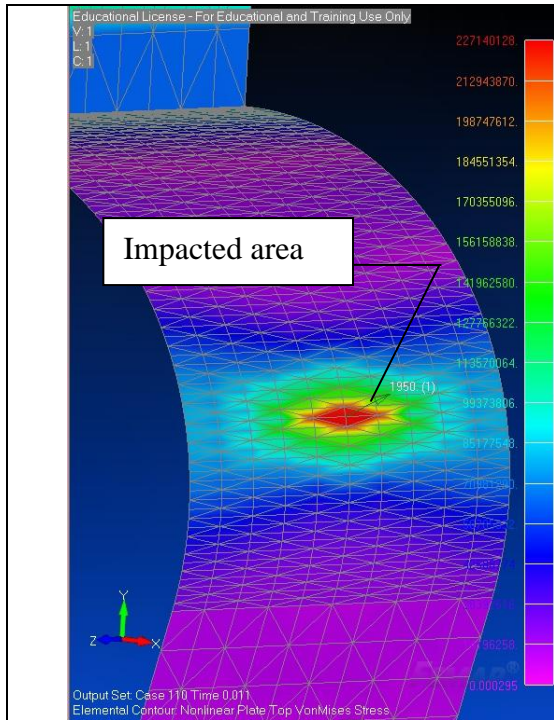


**Fig.2.8.** Detail of the impacted area (valid for both simulated models)

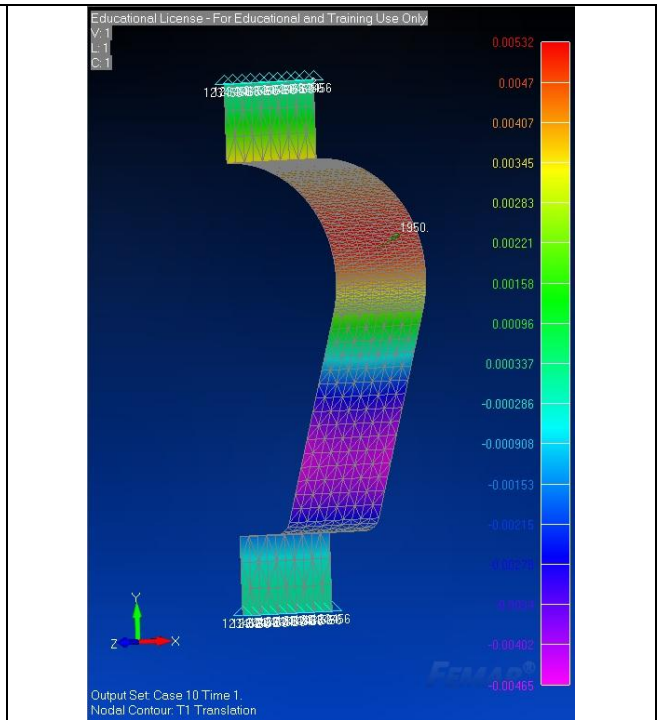


**Fig.2.9.** Displacements of the points on the X axis, in the model plate 1 with the maximum value in node 523, non-linear static analysis

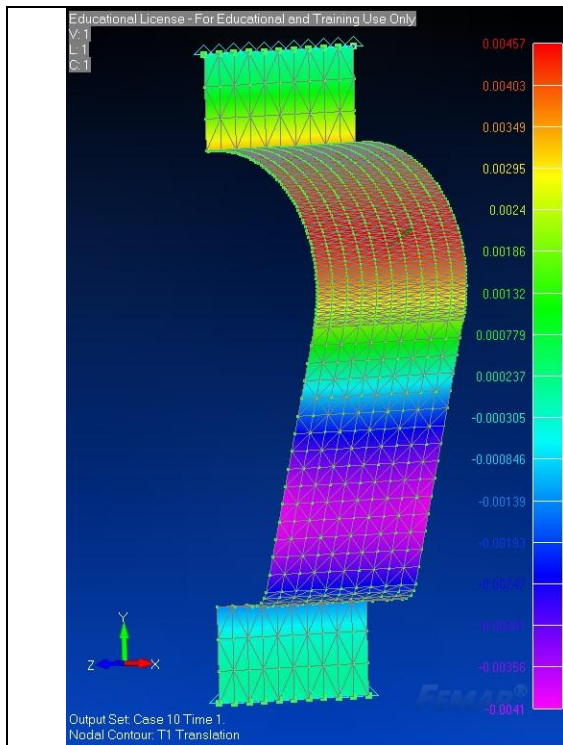


**Fig.2.10.** Displacements of the points on the X axis, in the model plate 2 with the maximum value in node 497, non-linear static analysis

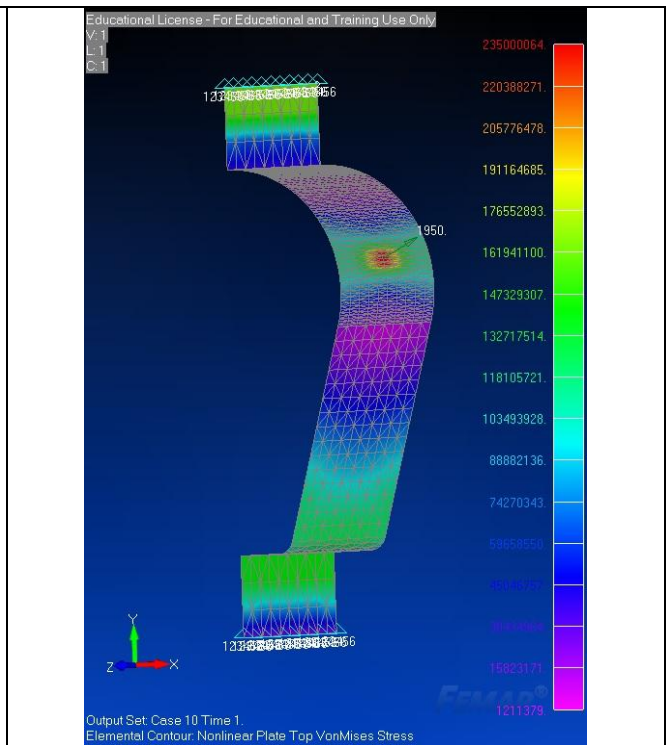


**Fig.2.11.** Von Mises stress for model 1 with maximum value on element 684, non-linear static analysis



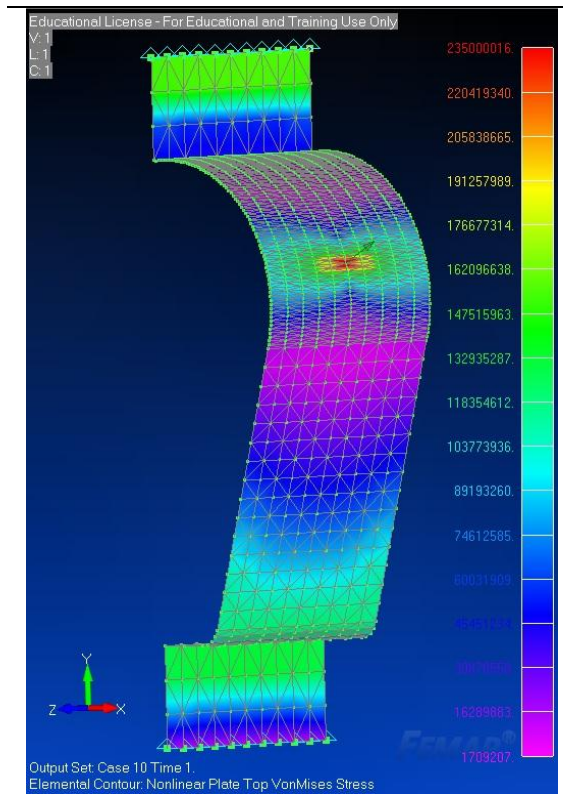


**Fig.2.12.** Von Mises stress for model 2 with maximum value on element 680, non-linear static analysis

*b) Dynamic numerical simulation of the impact in the application FEMAP 11.4*

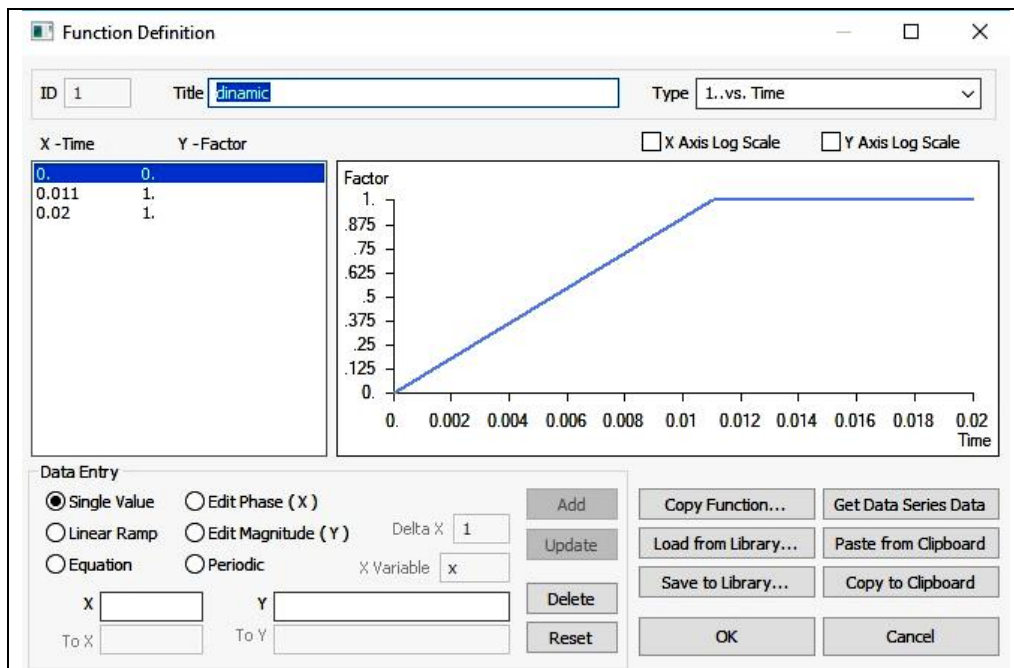


**Fig.2.13.** Description of the load factor of the time function, after T = 11ms, this being constant

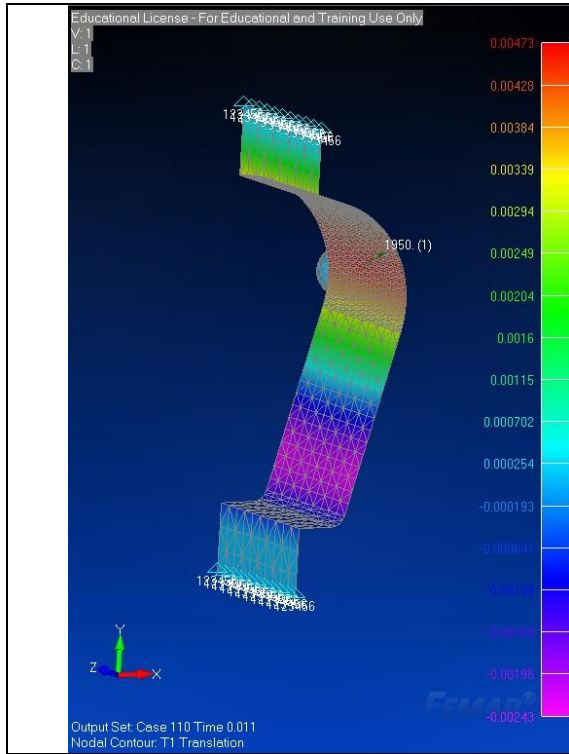


**Fig.2.14.** Displacements of the points on the X axis, in the model plate 1 with the maximum value in node 523, explicit dynamic non-linear advanced analysis

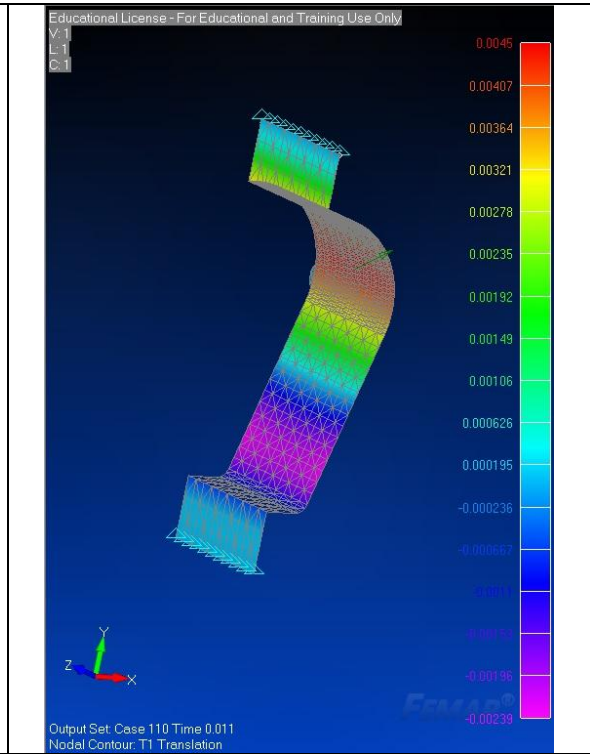


**Fig.2.15.** Displacements of the points on the X axis, in the model plate 2 with the maximum value in node 497, explicit dynamic non-linear advanced analysis

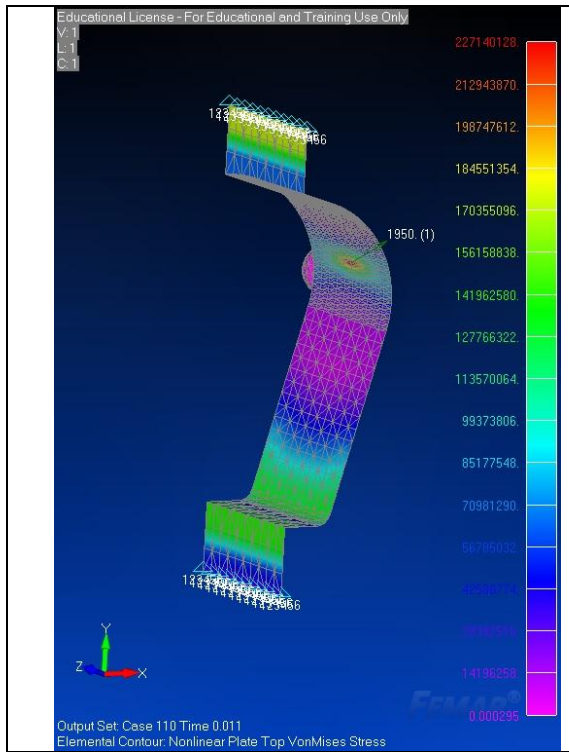


**Fig.2.16.** Von Mises stress for model 1 with maximum value on element 684, explicit dynamic non-linear advanced analysis

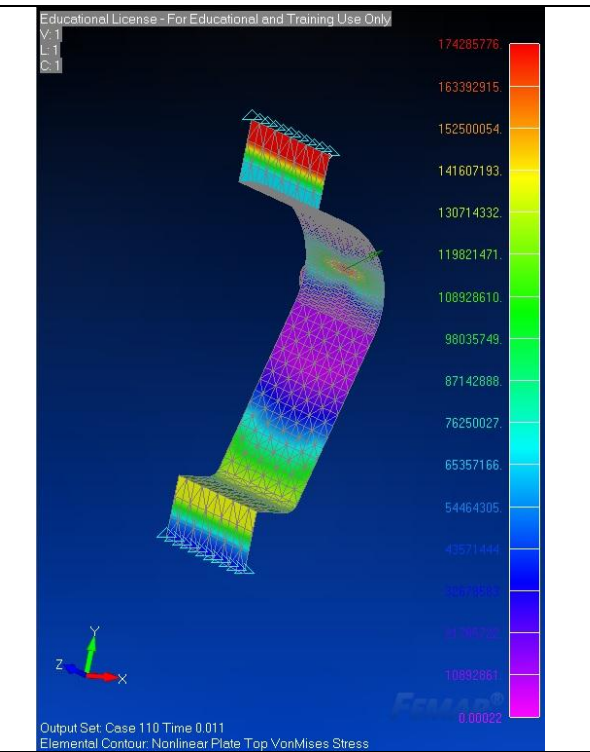


**Fig.2.17.** Von Mises stress for model 2 with maximum value on element 680, explicit dynamic non-linear advanced analysis



For the correct evaluation of the impact behavior of the two plates, the deformation energies specific to the static non-linear analysis were calculated.

**2.2. Data analysis on the influence of geometry on the stress and deformation**

In Table 2.6 it is observed that the value obtained in the static numerical simulation, realized for model 2, is lower for the maximum displacement of the impacted node, while the deformation energy is higher.

**Table 2.6.** *The results of the impact research using static numerical simulation in Femap 11.4*

<b>Object</b>	<b>Displacements (mm)</b>	<b>Von Mises Stress (MPa)</b>	<b>Energy (J)</b>
Model 1	5.01	235	4.85
Model 2	4.22	235	5.01

The numerical values obtained in the static non-linear finite element analysis, presented in Table 2.7, are comparable to the experimental ones being included in an accepted range, 6.187% for model 1 and 8.293% for model 2.

In explicit non-linear similar results were obtained, 5.588% for model 1 and 6.635% for model 2.

**Table 2.7.** *Displacements for an impact with F = 1950 N*

Model	<b>Maximum node displacement (mm)</b>		
	Aramis HS	Femap 11.4	
		Nonlinear analysis type	
		Static	Explicit
1	5.01	5.32	4.73
2	4.22	4.57	4.5

The influence of the curvature on the models behavior under impact loads is mentioned in Table 2.8.

**Table 2.8.** *Analysis of the shape influence on the behavior of the curved plate under impact loads*

<b>Analisis Type</b>	<b>Response</b>	<b>Variation of the response of model 2 vs. model 1 (%)</b>
Aramis HS	Deformation	-15.76
Femap 11.4	Deformation	- 4. 86

### 2.3. Concluding remarks

In the comparative study of the experimental research using the non-linear static numerical simulation it is observed that the decreasing modification of the curvature for the model 2, which registers an increase of the radius by 6%, shows:

- decrease of deformations by 15.76% experimentally, 14.09% for non-linear static numerical simulation and 4.86% for nonlinear explicit numerical simulation;
- 1.25% increase in mass

These conclusions are favorable to the choice of the curvature change procedure used in model 2, for generating the new geometries of the 2000 TDW barge board shells. Non-linear explicit analysis is used to study the dynamics of von Mises stress, for comparative study of the impact behavior of structures.

## CHAPTER 3

### PRELIMINARY STUDY OF A NAVAL STRUCTURE UNDER IMPACT LOADS

#### The objectives of this chapter are:

1. pre - processing of data for the naval structure's numerical model implementation;
2. finite element structural analysis of the numerical model under impact loads;
3. post- processing of data;
4. identification of the parameters that influence the impact phenomenon.

In the naval field, the impact phenomenon is regulated by the norms included in DNV GL-RP-204 [51] issued in 2017, which standardizes design that ensures the safety of the ships operations in case of accidental loads of their structure. This phenomenon is verified, both for objects falling in the air, on deck or in water (drop test) and for collisions of ships.

This chapter presents the structural analysis of a naval structure, with the purpose of verifying it at the impact on the deck using kinetics energy of 100 kJ. The impact was obtained by the free fall of a mass  $m = 2000$  kg, with the velocity  $v = 10$  m / s, from a height  $h = 5$  m / s, the gravitational acceleration being  $g = 9.81$  m / s<sup>2</sup>. The model processing is fully realized with the NX NASTRAN FEMAP 11.4 software application.

#### 3.1. Preliminary study of a naval structure for structural analysis

The data preparation stage for performing a finite element structural analysis is known as the data pre-processing stage. It comprises the phases of realization, both of the geometry of the CAD model and of the finite element model. The physical model is implemented in the digital environment either by scanning or by the physical object's representation in a CAD software (AutoCAD, etc.), being the source to achieve the finite element model.

##### 3.1.1 Geometric modeling of a naval structure (CAD Method)

3D modeling of the B2000T barge's geometry was performed, using dimensional data existing in the technical documentation designed in 1985 by ICEPRONAV Galați (the collective from Brăila), the general data [52] being mentioned in Table 3.1.

**Table 3.1.** General design data for the B2000T barge [52]

Nr.	General data	Symbol	Design data
1	Length over all	$L_{OA}$	76.18 m.
2	Length between perpendiculars	$L_{pp}$	75.72 m.
3	Breadth	B	11.00 m.
4	Draft	T	3.02 m.
5	Intercostal distance		0.50 m.
6	Water line distance		0.50 m.
7	Displacement	$\Delta$	338 t.
8	Deadweight	TDW	2000 t.

CAD model is only a portion of the bow, located between the watertight bulkhead C120 and the watertight bulkhead of the chain locker, which starts at frame C126. It includes the shell of the main deck and the board to the hardened area, 3.6 m from the main deck. The deck is reinforced with 7 deck's transverse beam and 3 deck's longitudinal, the last two arranged symmetrically to the one in the midplane. The border is reinforced with 7 frame, from C120 to

C126, C120 being the last frame of the cylindrical area. Table 3.2. records the design data of the structure realized in a transverse frame system.

**Table 3.2.** General design data for the CAD model of the barge

Nr.	Structure elements	Dimensions (mm)
1	Deck shell	8
2	Board shell	6
3	Deck's transverse beam	L 80 x 65 x 10
4	Deck's longitudinal stiffeners	T 200 x 80 x 6
5	Board stiffeners	L 80 x 65 x 6
6	Intercostal distance	500
7	Distance between longitudinals	1994 to stern and 1850 to bow

The commands of the Geometry and Modify menus [53] are used to create the CAD parasolid model. The CAD modeling phase is completed after checking the contacts between the structure elements. The lack of links between the elements of the geometry is complemented by new curves, for the connection between bridges, sleepers and ribs. The lack of connections between the elements of the geometry determines its completion with new curves, in order to achieve the connection between the components of the structure.

### 3.1.2 Structural modeling of a naval structure's geometry (Finite Element Method)

To perform a structural analysis it is necessary to execute the discretization of the geometry surfaces using the finite element method. Impact is a complex, non-linear phenomenon for both bodies in contact. It was considered that the material subjected to the impact loads is a plastic-non-linear material, with kinematic hardening, defined by a stress-strain curve, with the properties recorded in Table 3.3.

**Table 3.3.** Properties of non-linear plastic material

Nr.	Material properties	Units	Naval structure	Striking object
1	Thickness	mm	see Table 3.2	120
2	Young modulus	MPa	$2.1 \times 10^5$	
3	Poisson coefficient	-	0.3	
4	Density	tone /mm <sup>3</sup>	$7.85 \times 10^{-9}$	
5	Yield stress	MPa	236.2	
6	Ultimate limit stress	MPa	432.6	

For modeling, plate elements, CQUAD4 with Kirchoff theoretical formulation, were initially chosen.

Some of the elements were modeled with CTRIA3 type elements, with the triangular shape that allowed, for certain parts of the curved plate, to achieve contact between the structure elements.

The quality of the mesh, in particular its density, affects the results of structural analysis [54]. Naval mesh elements have to comply with DNVGL-LP-0127 [55] which is considered quality items. The NX NASTRAN FEMAP software allows the comparison of the elements with the type of initially chosen element, through a series of indicators (flatness, proportion, distortion, explicit time step, etc.).

The most important indicator is the Jacobian determinant by which the deviation of the shape of the element from an ideal shape is verified, with accepted values between 0 and 1. For the two bodies subject to the impact, these indicators were checked, obtaining for the naval structure, a Jacobian = 0.860 and valid values for the impact area (Jacobian = 0.52, aspect ratio = 2.44 and warping =  $1.2 \times 10^{-6}$ ).

The naval structure was impacted on deck by a striking object composed of a hemisphere and a cylinder having the design data specified in Table 3.5. The material properties are mentioned in Table 3.3.

**Table 3.5.** Design data of the striking object's geometry

Nr.	Object	Dimension	Units
1	Hemispherical radius	300	mm.
2	Cylinder	700	mm.

### 3.2. Structural analysis of a naval structure under impact loads (Finite Element Method)

The impact phenomenon was modeled using dynamic software analysis, called Advanced Nonlinear Explicit. The contact has been simulated by the non-linear correction method, defining the regions. For the behavior's study using numerical analysis of a naval structure under impact loads, experimental data are used in the literature [46, 56]. In this paper, the friction coefficient values are chosen from the scientific literature studying the impact of naval metal structures [6].

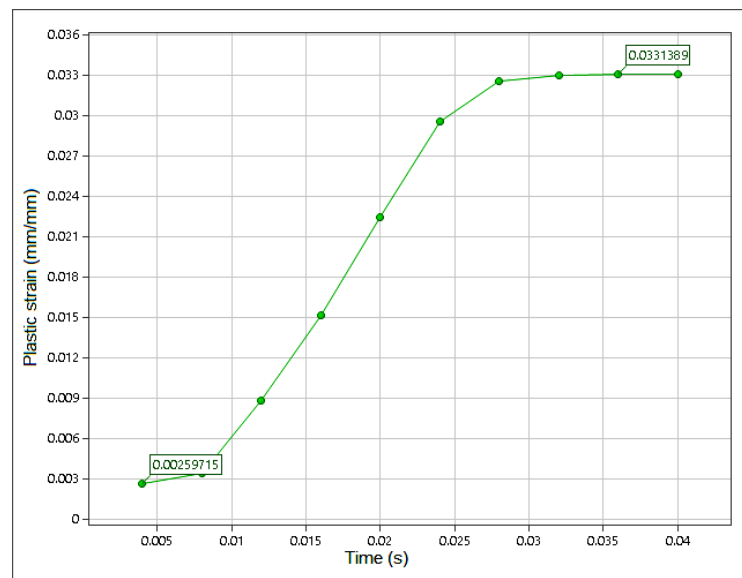


**Fig. 3.9.** Variation of the plastic strain of the deck, element 140,  $T = 40\text{ms}$ ,  $\mu = 0.6$ .

The structures of the barge not included in the structural analysis were represented by border conditions, by blocking the displacements along X and Y axis, and rotation around Z axis. In order to determine the duration of the analysis, the software run for 40 milliseconds was initially performed. The plastic strain presented in diagram of Fig. 3.9 shows that this deformation stagnates after 32 milliseconds.

Running time  $t = 40\text{ms}$  was chosen for three analyzes using the material properties, presented in Table 3.6., with values of the friction coefficient parameter.

**Table 3.6.** Properties of material S235 according to DNV-GL [57]

Nr.	Strain (mm/mm)	Stress (MPa)
1	0	0
2	0.004	236.2
3	0.0198	243.4
4	0.1817	432.6

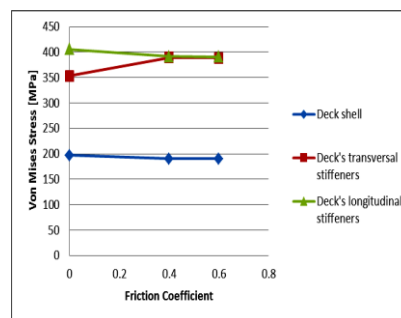
### 3.3. Data post-processing

The maximum values for total displacements, Von Mises stress and shear stresses were determined

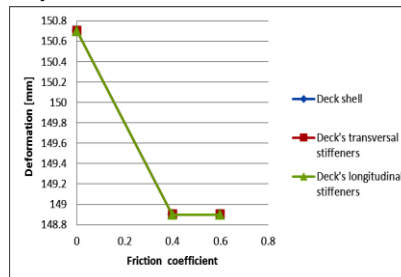
The analyzed results, for each component of the naval structure impacted in node 150, element 140, after the completion of the impact, are presented in a table. Analyzing the results, we observe an influence of the coefficient of friction on the stresses that appeared in the structure following the impact, recorded in the label a) of Fig. 3.17.

In this diagram, on the abscissa, the values of the friction coefficient are recorded and on the ordinate the values of the Von Mises stress of the impacted structure. The same reasoning also applies to label b) of Fig. 3.17, where the values for the deformations in the structure are illustrated.

The striking object caused a plastic strain of the deck, for the friction coefficient,  $\mu = 0.6$ , with the value 0.0331 mm / mm. This is accepted, according to the rules of the classification company DNV GL [58], the naval structure shows safety in navigation following the presented impact.



a) Von Mises stress variation



a) Variation of deformations

**Fig. 3. 17** The influence of the friction coefficient on the stress and deformations variations resulting after the impact on the naval structure with E = 100 kJ (v = 10 m / s)

### 3.4. Concluding remarks

The following conclusions are drawn using the data analysis from label a) and b) of Fig. 3.17:

1. The finite elements defining the naval structure and the striking object comply with the numerical modeling norms prescribed in DNVGL-CG-0127.
2. The impact of the naval structure with an energy of 100 kJ ( $v = 10\text{m} / \text{s}$ ) causes structure's changes, respectively a deck's plastic strain value of 0.0331 mm / mm, for  $\mu = 0$ , allowed by the norms of the classification societies, which accepts maximum 5 % for this criterion.
3. Friction influences the impact phenomenon only by including it in the analysis, less by the value of the coefficient of friction.
4. The friction coefficient has a small influence on the deformations of the elements of the impacted structure, these being equal to each other, with the value 148.9 mm, for both friction coefficients.
5. The friction coefficient influences the magnitude of the Von Mises stress, the largest being on the longitudinal and the smallest on the deck, 391.6 MPa, respectively 190.3 Mpa, for  $\mu = 0.4$ .
6. The friction coefficient influences the magnitude of the shear stresses, the largest being on the longitudinal and the smallest on the deck, 218.6 MPa, respectively 93.09 Mpa, for  $\mu = 0.4$ .
7. The friction coefficient reduces the deformations by 1.19% for all the elements of the structure, for both friction coefficients.
8. The friction coefficient determines both the decrease of the Von Mises stress for the deck and the longitudinal ones, as well as the increase of the stress for the deck's transverse beams, the highest influence being on the deck's transverse beams and the smallest on the deck, with 10.4% for  $\mu = 0.4$ , respectively 3.25% for  $\mu = 0.6$ .
9. The frictional coefficient causes both the decrease of shear stresses for the deck, as well as the increase of the stresses for the longitudinal and transverse beams, the greatest influence being on the longitudinal and the smallest on the deck, with 11.1% for  $\mu = 0.4$ , respectively 0.08% for  $\mu = 0.6$ .

These conclusions are favorable to the use of the friction coefficient, as a parameter of the collision analysis, to study the influence of the geometry of the B2000T barge, loaded at traction and bending during impact.





**CHAPTER 4****STUDY OF THE INFLUENCE OF GEOMETRY ON THE STRESSES OF NAVAL  
STRUCTURE UNDER IMPACT LOADS**

**The objectives are as follows:**

1. studying the influence of the friction on the side impact of a naval structure;
2. study the influence of geometry on the stresses resulting from impact;
3. finding ways to reduce stress Von Mises results during impact.

River navigation currently holds a significant share of all freight transport, in central Europe this being one third of the total traffic [59, 60]. In 2011, on the Danube River included in the Pan-European Corridor VII, Romania accounted for 58.4% of the total freight transport on waterways [61]. These activities may be disturbed by ship accidents due to the impact with floating wooden hubs or with the supporting elements of the bridges [62, 63, 64], or the adverse weather conditions that may cause the damaged barges.

In order to design a ship structure with high impact resistance, this chapter presents the simulation of a side collision with energy of 1 kJ. The side impact of the board's structure impacted with a mass  $m = 2000$  kg, with the speed  $v = 1$  m / s., was done. The model simulation is fully realized with the NX NASTRAN FEMAP 11.4 software application [65, 66].

**4.1. Study on a naval structure under side impact loads****4.1.1. The impact's selection procedure for a naval structure**

The behavior of the structure at impact load was studied by placing the striking object on a perpendicular direction to the barge's midplane, at three points of the board with different curvatures of the frames. Numerical structural analysis uses both the geometric model of the naval structure and the striking object, described in Chapter 3, with the same material properties. A side collision, on the starboard is done.

The numerical model of the impacted surface, composed of the board and the corresponding frames is made with the finite element method whose mesh quality is presented in Table 4.1, in compliance with the norms DNV-GL-RP-C208 [57].

**Table 4.1.** Variation of the elements quality in the impacted area

Impacted area	Mesh Quality	
	Jacobian	Aspect ratio
Board	0.597	3.035

**4.1.2. A model structural analysis under impact loads**

The naval structure is impacted with an energy  $E = 1$  kJ, resulting from the collision of the striking object that have a mass = 2000 kg, with the speed  $v = 1$  m / s. Impaction is performed in three points with different curvature of the starboard shell, below the latest waterline (at = 3 m. to the base plane, on the bottom of the barge). The impact points are chosen at the frames C121, C123 and C125, the lowest curvature being at frame C121.

The analysis is carried out for a time  $T = 40$  ms, until the completion of plastic strain indicated by a constant value thereof, as exemplified in Fig. 4.2.

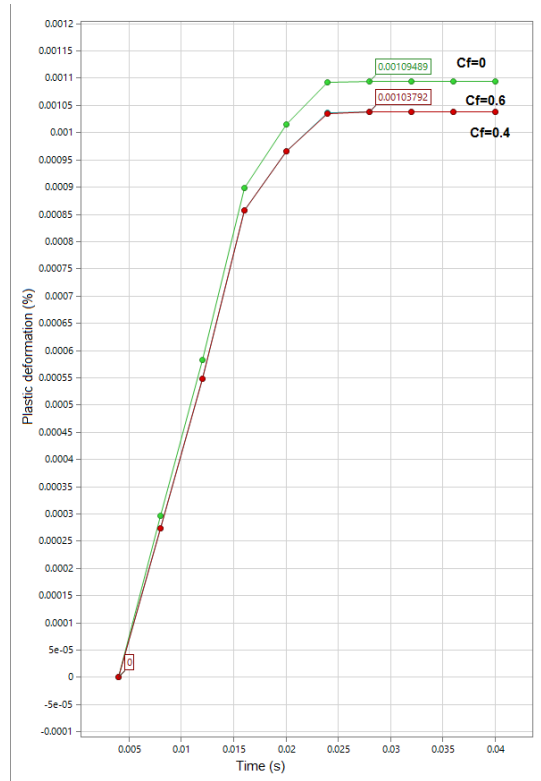


**Fig. 4.2.** Variation of plastic strain for frame C121 (x=64.62 m, y=3.19 m, z= 5.49 m), T = 40 ms

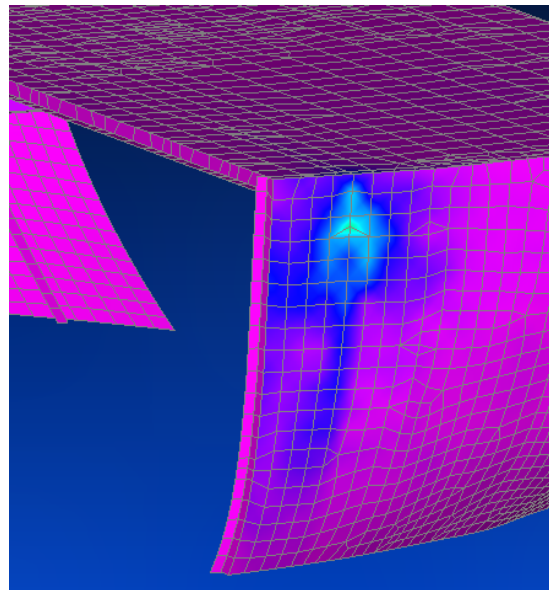


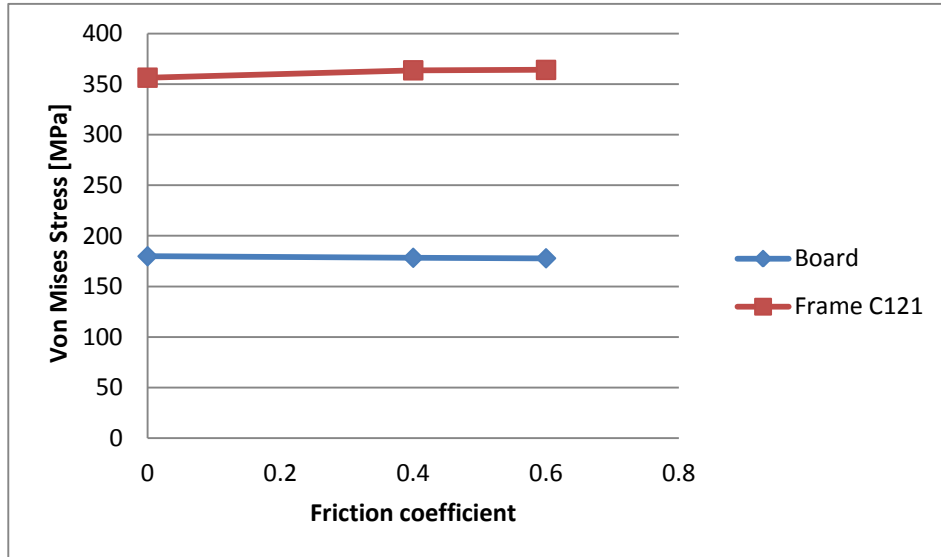
**Fig. 4.3.** Variation of the Von Mises stresses of the impacted board at the frame C121 with E = 1 kJ, analyzed for t = 40 ms,  $\mu = 0.6$

It can be seen from Fig.4.3 that the impact phenomenon was locally manifested, around the point of impact, on the board and the frame. The response of the structure on the deck is minor, the effects of the collision manifesting, in intensity, more on the frame, while on the board the surface affected by the impact is greater.

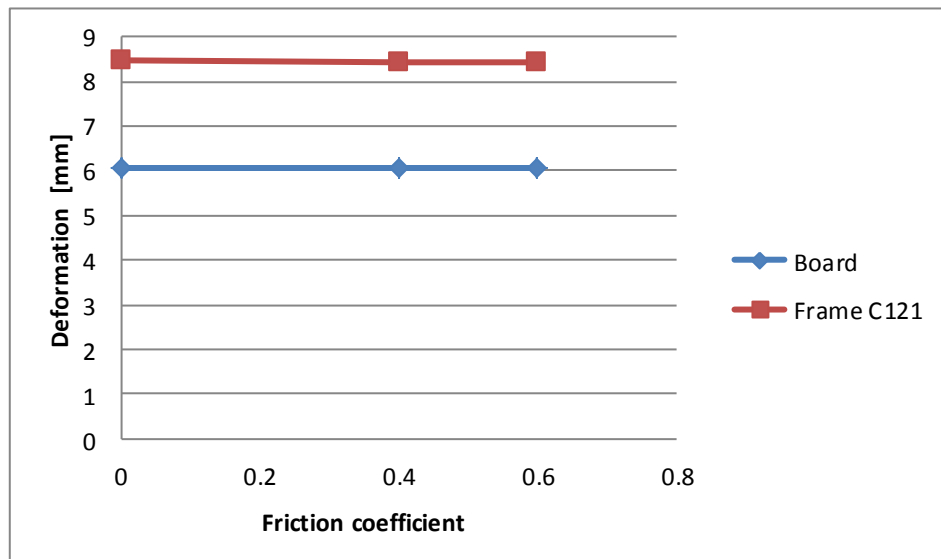
After the completion of the impact, the analysis's results, for each component of the impacted naval structure, are presented in a table.

### 4.1.3. Data analysis

The presented data show the influence of the friction on the impact phenomenon, recorded in charts. In label a) of Fig. 4.9, on the abscissa, are the values of each friction coefficient and on the ordinate the values of the Von Mises stresses in the structure, at the frame C121.



a) Von Mises stress variation



b) Variation of deformations

**Fig. 4.9** The influence of the friction coefficient on the stress and deformations variations resulting after the impact on the naval structure with  $E = 1 \text{ kJ}$  ( $v = 1 \text{ m / s}$ ) at the frame C121 ( $x = 64.62 \text{ m}$ ,  $y = 3.19 \text{ m}$ ,  $z = 5.49 \text{ m}$ )

The same reasoning also applies to the label b) of Fig. 4.9 where the values for the deformations in the structure, at the frame C121, are illustrated. The charts also are done to show similar results for frames C123 and C125.

It is observed that the value of the friction coefficient causes the decrease of the total deformation values of the board and the frames nodes, the influence being greater on the

board. The deformations have identical values for the both variants of the parameter, for each of the analysed components, except for the values corresponding to board at the frame C121.

The presence of friction causes both the decrease of the Von Mises stresses on the board at frames C121 and C125, on the frame C123 and the increase of the stresses on the frames C121 and C125 and on the board at the frame C123, with a greater influence on the board at the frame C125 and on the frame C121.

This parameter influences the shear stresses, which have high values corresponding to the frame C121 and the board at frame C125.

**4.2. Study of the influence of geometry on the stresses under impact**

The study of the influence of geometry on the stresses due to the side impact is performed by analysing the Von Mises stresses that appeared in the elements of the board, impacted at the frames C121, C123 and C125, presented in the tables of paragraph 4.1.2. Fig. 4.12 illustrates the variation of Von Mises stresses along the board, the origin being at the frame C121, the other frame being at an intercostal distance equal to 500 mm.

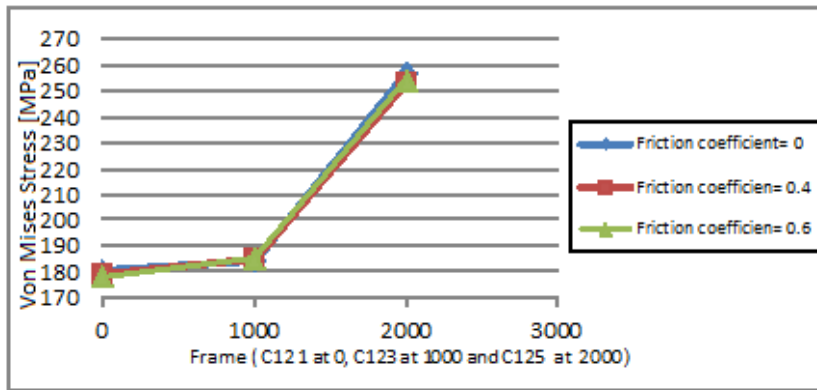


**Fig. 4.12.** The influence of geometry on Von Mises stresses for impacted board with  $E= 1 \text{ kJ}$  ( $v=1\text{m/s}$ ), at frames C121, C123 and C125

An increasing of Von Mises stress from 177.8 MPa, is observed for the elements on a surface with a small curvature, near the cylindrical area positioned at C120, towards the bow, characterized by a larger curvature corresponding to frame C125, where the maximum value 254 MPa, for  $\mu = 0.6$ , is obtained.

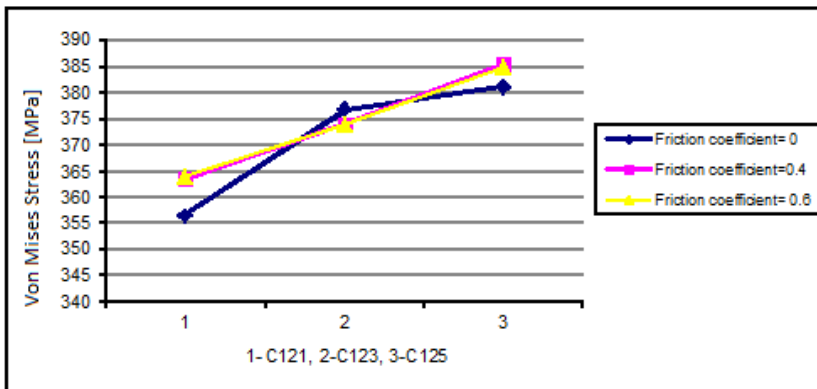


**Fig. 4.13** The influence of geometry on Von Mises stresses for impacted frames with  $E= 1 \text{ kJ}$  ( $v=1 \text{ m/s}$ ), at frames C121, C123 and C125

Similarly, an increase of Von Mises stress is observed, towards the bow, from the frame C121 to C125, respectively from 364 MPa to 384.7 MPa, illustrated in Fig.4.13. The trend to increase stress is observed in the diagram of Fig. 4.14, that show the results of the side impact of the board at the frame C124, located between C123 and C125, under similar analysis conditions to the other 3 numerical simulations.

The curves in Fig. 4.14, drawn for the both friction coefficients, 0.4 and 0.6 respectively, more accurately illustrates the increase of stresses as a function of the increase of curvature along the X axis, towards the bow.

Fig 4.15.a shows the influence of the curvature of the board on the Von Mises stresses expressed as a percentage in Table 4.9, with their variations with respect to the frame C121.

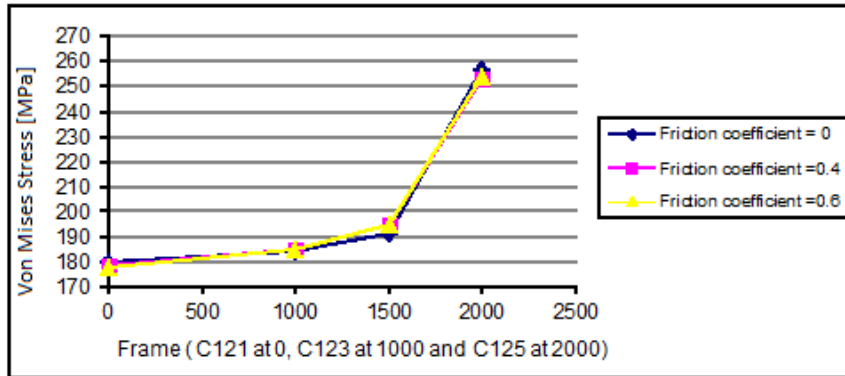
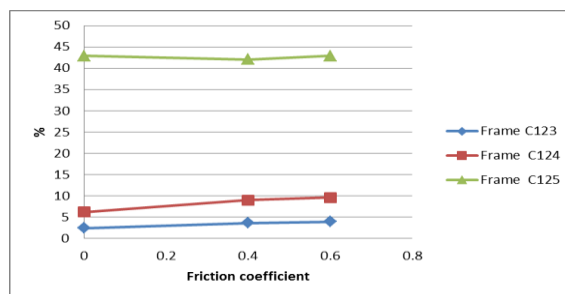


**Fig. 4.14.** The influence of geometry on Von Mises stresses of the impacted board with  $E = 1 \text{ kJ}$  ( $v = 1 \text{ m / s}$ ), at the frames C121, C123, C124 and C125

**Table 4.9.** Relative variation of Von Mises stresses of the board with respect to frame C121 ( $x = 64.62 \text{ m}$ ,  $y = 3.19 \text{ m}$ ,  $z = 5.49 \text{ m}$ )

Friction coefficient, $\mu$	C123	C124	C125
0.	2.44	6.17	42.88
0.4	3.58	8.97	42.06
0.6	3.93	9.61	42.85
The distance on the X axis from frame C121, as its origin, to the bow (mm.)	1000	1500	2000



**a)** Von Mises stress variations expressed as a percentage against frame C121

**Fig. 4.15.** The influence of the geometry on the Von Mises stresses and deformations variations of the board, as a function of the friction coefficient

### 4.3. Variants of diminishing Von Mises stress under impact loads

Fig.4.12, Fig. 4.14 and Fig. 4.15.a show an increased value for Von Mises stress, as a result of the impact of the board on the frame C125. In order to diminish this effect, it is necessary to choose a new geometry, by modifying the geometrical characteristics of the structure, in order to keep the ship in operation after impact. Based on the results of the presented simulations, it is proposed a way to change the thickness of the structure board in the impact area. This represents a solution without major consequences, from a hydrodynamic point of view, the correction of the trim due to the mass increasing can be quickly done.

**Table 4.10.** Variants of redesigning the geometry of the naval structure

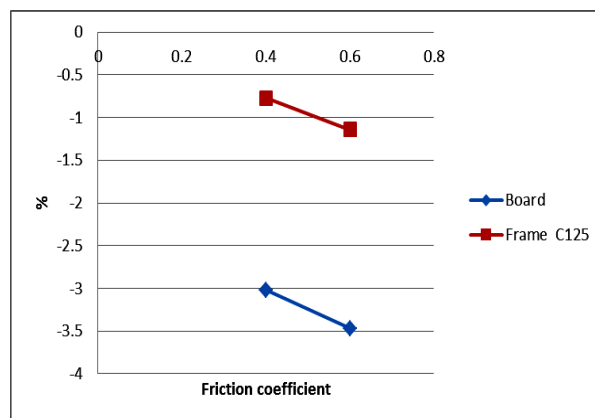
Nr.	Variant	Shell thickness (mm)		Structure mass (tone)	Changed mass (%)
		Board at frame C125	Frame C125		
1	initial	6	6	4.644	-
2	I	6	7	4.751	2.30
3	II	7	6	4.896	5.42

The solution for increasing the thickness of the shell is illustrated in Table 4.10. that presents the both variants of thickness modification, corresponding to the frame C125 for variant 1, and changes of the board's thickness at the frame C125, for variant II. Changes in the mass of the naval structure by 2.30 %, respectively 5.42 % compared to the initial mass do not produce major changes in the buoyancy of the barge.

Data recorded in the table were obtained from the structural impact analyzes, performed under similar simulation conditions, for the both variants of the modified geometries.

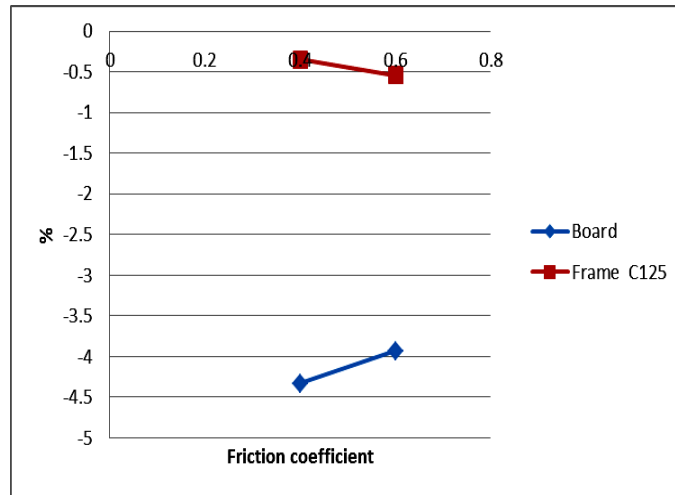
#### 4.3.1 Studying the influence of friction on the side impact of naval structures with redesigned geometry

The analysis of the data presented in the table shows the influence of friction on the impact phenomenon, recorded as a percentage in the label a) of Fig. 4.16 and Fig. 4.17, for the both variants of the new geometries, according to the data from Table 4.10.



a) Von Mises stress variation

**Fig. 4.16.** The influence of the friction coefficient on the Von Mises stress resulting after the impact on the naval structure with E = 1 kJ (v = 1m / s) at the redesigned frame C125 (Variant I)



a) Von Mises stress variation

**Fig. 4.17** The influence of the friction coefficient on the Von Mises stress resulting after the impact on the redesigned naval structure with  $E = 1 \text{ kJ}$  ( $v = 1 \text{ m / s}$ ) at the frame C125 (Variant II)

It is observed that the value of the friction coefficient causes the decrease of the Von Mises stress values of the board and the frame's nodes, the influence being greater on the board in the variant of the redesigned frame C125. The presence of friction determines the decrease of Von Mises stress for the board and the frame C125, with a greater influence on the elements of the redesigned board.

This parameter influences the shear stresses, by lowering them, with higher values for the redesigned board, corresponding to frame C125.

#### 4.3.2 Studying the influence of the redesigned geometry on the stresses under impact loads

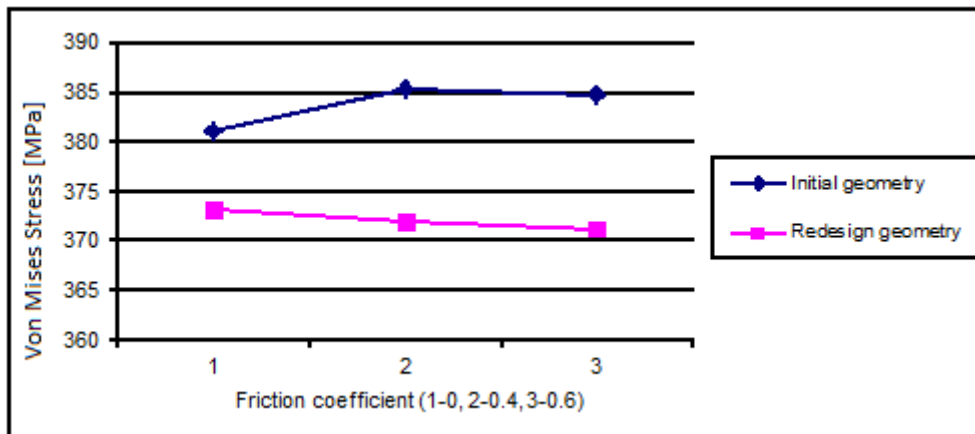


**Fig. 4.18.** Comparative study of the influence of the friction coefficient on the Von Mises stresses of the frames for the both variants of geometries

Analysing the table data, it can be seen that the Von Mises stresses are further reduced for the elements of the C125 coast, for variant II, where the thickness of the border has been changed by 1 mm, corresponding to this coast. In Fig. 4.18 is observed that these stresses decrease for the redesigned geometry regardless of the friction coefficient's value.

Fig 4.19 shows the percentage values of the Von Mises stresses that decrease for the modified geometry compared to the initial geometry.

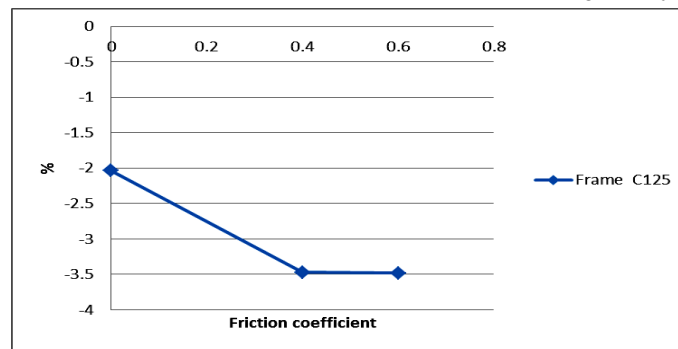


**Fig. 4.19.** Comparative study of the influence of geometry on the Von Mises stresses for the frame C125 (Variant II)

#### 4.4. Concluding remarks

From the numerical analysis, including the friction during the side impact of the starboard of the naval structure with an energy  $E = 1$  kJ ( $v = 1$  m / s), positioned at three points with different curves of the board, below the level of the last waterline at  $Y = 3$  m, the following conclusions were reached:

1. The friction coefficient's value determines the decrease for the values of the nodes' total displacement on the board and on the frame, the influence being greater on the board.
2. The total deformations have identical values for the both variants of the parameter, for each of the analyzed components, except for the board's values corresponding frame C121.
3. The presence of friction determines both the decrease of the Von Mises stresses for the board at frame C121 and C125, for the elements of the frame C123 as well as the increase of the stresses on the elements of the frame C121 and C125 and the board at frame C123 - a greater influence is manifested on the board at frame C125, with -1.40% and on frame C121 with cu 2.16%.
4. The coefficient of friction influences the shear stresses, with the maximum increase of 2.33% corresponding to the elements of the frame C121 and with the maximum decrease of 2.32% for the elements of the board at the frame C125.
5. Von Mises stresses increase with increasing curvature along the board toward the bow, from 177.8 MPa at frame C121 to 254 MPa at frame C125, for  $\mu = 0.6$ , representing an increase of 42.85%.
6. Von Mises stresses increase with increasing of the curvature of the frame towards the bow, from the value of 364 MPa at the frame C121 to the value of 384.7 MPa at the frame C125, which represents an increase of 5.68%.
7. The increase of the thickness of the boards (from 6 mm to 7 mm) by 16.6% causes a decrease of the Von Mises stresses of 3.47% of the frame C125 compared to the similar values of the frame C125 of the initial geometry (variant II).
8. Increasing the thickness of the board (from 6 mm to 7 mm) by 16.6% causes a decrease of 3.68% for Von Mises stresses for the frame C125 compared to similar values for the frame C121 (variant II).

In this study, conclusions were drawn regarding the state of deformation when reaching the plastic deformation stage.



## CHAPTER 5

### STUDY OF THE GEOMETRY'S INFLUENCE ON A STRUCK NAVAL STRUCTURE'S RUPTURE

#### Chapter objectives are:

1. carrying out scenarios for impacting the naval structure;
2. evaluation of the effects due to the impact (plastic strain, damaged volumes, dimensions of damaged areas);
3. geometry design solutions for diminish collision effects resulting in structure, after impact.

Due to the collisions of the ships, due to the high energies involved, the ships can be seriously damaged with the loss of safety regarding their navigation. Depending on the transported goods, which may be lost in the navigable channels, it can lead to environmental pollution. Even if there is a low risk coefficient for inland waterway accidents, the shipwreck may block the waterway, with great economic effects. Such a situation was created on September 2, 1991, with the shipwreck of the ship "Rostock" at mile 31 on the Danube, which sailed under the Ukrainian flag and blocked until 2005 the good sailing on the Sulina branch, being needed over 5,000,000 euros. for reactivating the channel. On June 29, 2003, the blocking of the Danube waterway was avoided at kilometer 361, where the impact of two barges took place. It was possible to avoid the shipwreck of the Bulgarian barge, due to the maneuvers performed by the commander of the "Tsar Kaloian" pusher who was sailing downstream, resulting in a rupture of the starboard barge of over 1 meter. The barge collided with a Romanian barge, accidentally detached from the Romanian convoy driven upstream by the "Cozia" pusher. Both barge convoys did not carry goods.

It can be observed that an analysis of the structure of the board's barge under impact loads may be a useful in order to improve the design of the geometry of its structure.

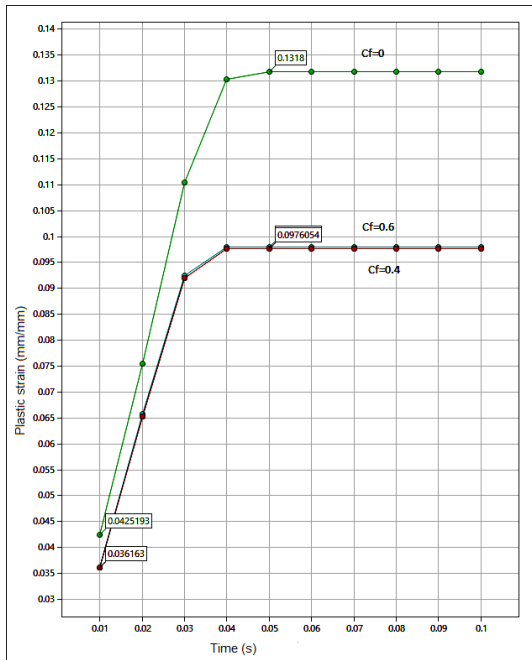
In this chapter is performed the structural analysis of a ship structure under impact loads to determine the influence of the geometry of the structure on its safety. 18 impact scenarios were realized, in 3 different points of the naval structure, described in chapter 3 (see §3.1) . The impact energies of 100 kJ and 400 kJ (C study) were simulated and generated by a striking object with a mass of 2000 kg. moving with 10 m / s, respectively 20 m / s, with different values of the friction coefficient. To study the variation of damage, the structure was impacted with the energy of 100 kJ and 144 kJ (D study), by the same striking object moving with 10 m / s and 12 m / s respectively. The collisions, analyzed by other 18 scenarios, are performed at the same points and under the same friction conditions, similar to the 18 scenarios previously described. In order to analyze the damage diminishing, 36 collision scenarios are done (variant I, variant II, variant III).

#### 5.1. Impact scenarios on the starboard of a naval structure

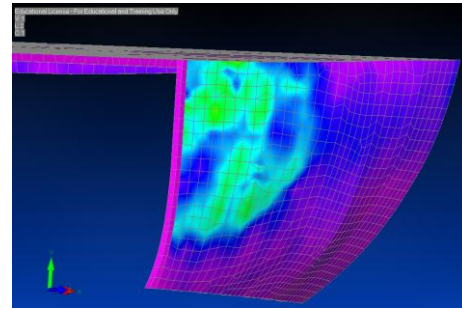
Numerical simulations were performed using the nonlinear finite element method to produce virtual experimental data for 18 collision scenarios of the ship structure.

##### 5.1.1. Evaluation of the effects due to the impact loads with 100 kJ

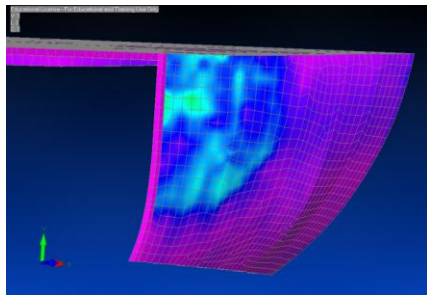
In Fig. 5.1 and Fig. 5.2 are presented variations of the plastic strain during the impact,  $T = 100$  ms, for the three variants of the coefficient of friction,  $C_f$ , for the impact of the structure on the frames C121 and C125, with the energy  $E = 100$  kJ.



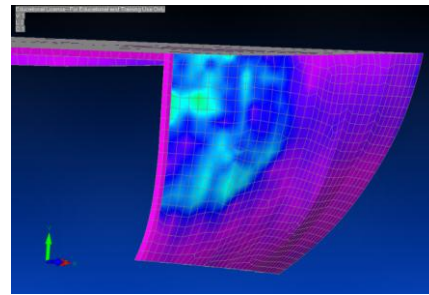
a) Variation of the plastic strain on the board for the element 4807



b) Von Mises stress variation on the board,  $\mu=0.0$



c) Von Mises stress variation on the board,  $\mu=0.4$



d) Von Mises stress variation on the board,  $\mu=0.6$

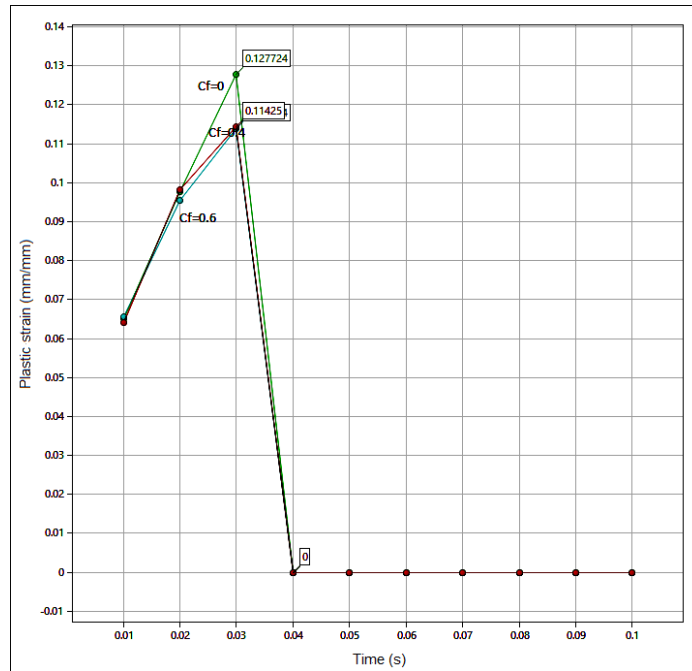
**Fig. 5.1** Variation of the plastic strain and Von Mises stress, for the impact on the structure at the frame C121 ( $x=64.62$  m,  $y=3.19$  m,  $z= 5.49$  m), with  $E= 100$  kJ ( $v=10$ m/s),  $T=100$  ms

In the label a) of Fig. 5.1 and Fig. 5.3 are shown diagrams of the plastic strain during the impact,  $T = 100$  ms, for the three values of the coefficient of friction,  $C_f$ , for the impact of the structure at the frames C121 and C125, with the energy  $E = 100$  kJ. We observe a different behavior of the structure depending on the curvature of the structure. Thus for a small curvature of the frame C121, located near of the cylindrical area, the constant value of the plastic strain, being constant, illustrates an impact at which the board does not break, for all 3 values of the coefficient of friction.

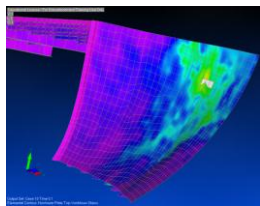
It is observed in the graph of label a) of Fig. 5.1, a decrease of the variation of the plastic strain by 25% for the cases in which the influence of friction was considered, at impact, compared to the case where the coefficient of friction was ignored. In variants b), c) and d) of Fig. 5.1, the behavior of the impact shell, at the end of the analysis, is illustrated for the three values of the friction coefficient.

The structure behaves similarly at the frame C123. The impact of the shell at the frame C125, located towards the bow, due to its curvature, determines the rupture of the shell, illustrated by the null value of the plastic strain at time  $T = 40$  ms, a phenomenon illustrated in label a) of Fig. 5.3 and labels b), c) and d) of Fig. 5.3, for the end of the analysis. It is observed

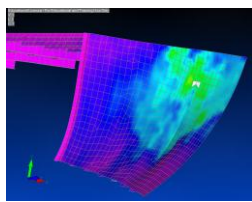
in the label a) of Fig. 5.3 a decrease of the plastic strain variation by 10% for the cases in which the influence of friction was considered, at impact, compared to the case where the friction coefficient was ignored. In the labels e), f) and g) of Fig. 5.3 the same damage of the impacted area is observed for all 3 values of the friction coefficient.



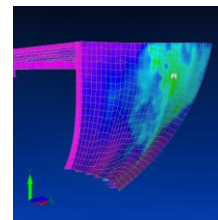
**a)** Variation of the plastic strain on the board for the element 4620



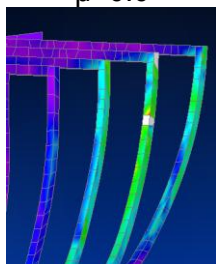
**b)** Von Mises stress variation on the board,  $\mu=0.0$



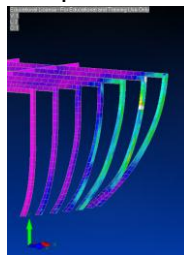
**c)** Von Mises stress variation on the board,  $\mu=0.4$



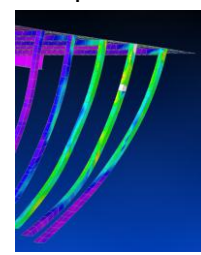
**d)** Von Mises stress variation on the board,  $\mu=0.6$



**e)** Von Mises stress variation on the frame,  $\mu=0.0$



**f)** Von Mises stress variation on the frame,  $\mu=0.4$



**g)** Von Mises stress variation on the frame,  $\mu=0.6$

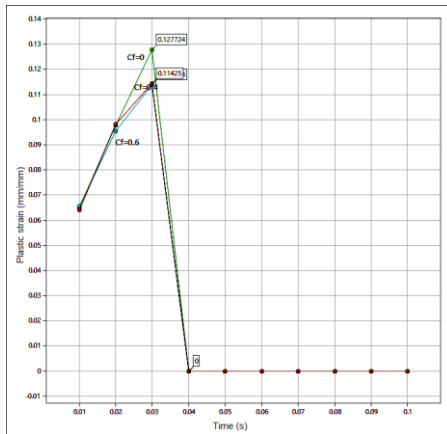
**Fig. 5.3** Variation of the plastic strain and Von Mises stress, for the impact on the structure at the frame C125 ( $x=66.62$  m,  $y=3.19$  m,  $z= 5.29$  m), with  $E= 100$  kJ ( $v=10$ m/s),  $T=100$  ms

An increase in damage is observed for the case where the friction is neglected, compared to the cases in which the influence of the friction is considered. Thus, three broken elements are identified, for the analyzes that consider the influence of the coefficient of friction, against two broken elements, for the analysis in which the friction phenomenon was ignored.

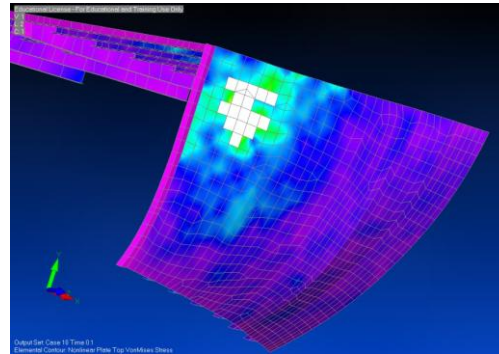
This causes a decrease in the variation of Von Mises stress by 6.60%, for the case of neglecting the friction compared to the case  $\mu = 0.4$ . Similarly, a decrease in the variation of Von Mises stress by 14.51% is identified, for the case of neglecting the friction, compared to the case  $\mu = 0.6$ .

5.1.2 Evaluation of the effects due to the impact loads with 400 kJ

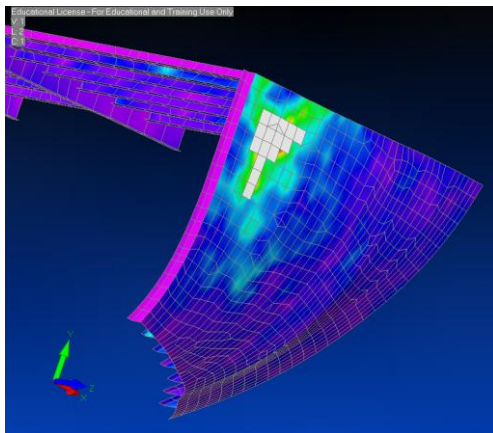
To study the influence of impact requests on the structure geometry, the impact speed was doubled, which resulted in an increase of energy from  $E = 100$  kJ to  $E = 400$  kJ.



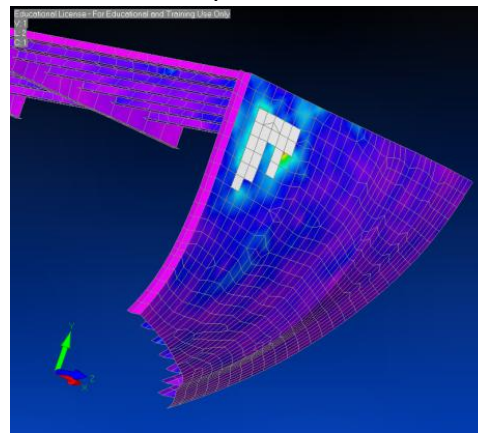
a) Variation of the plastic strain on the board for the element 4807



b) Von Mises stress variation on the board,  $\mu=0.0$



c) Von Mises stress variation on the board,  $\mu=0.4$



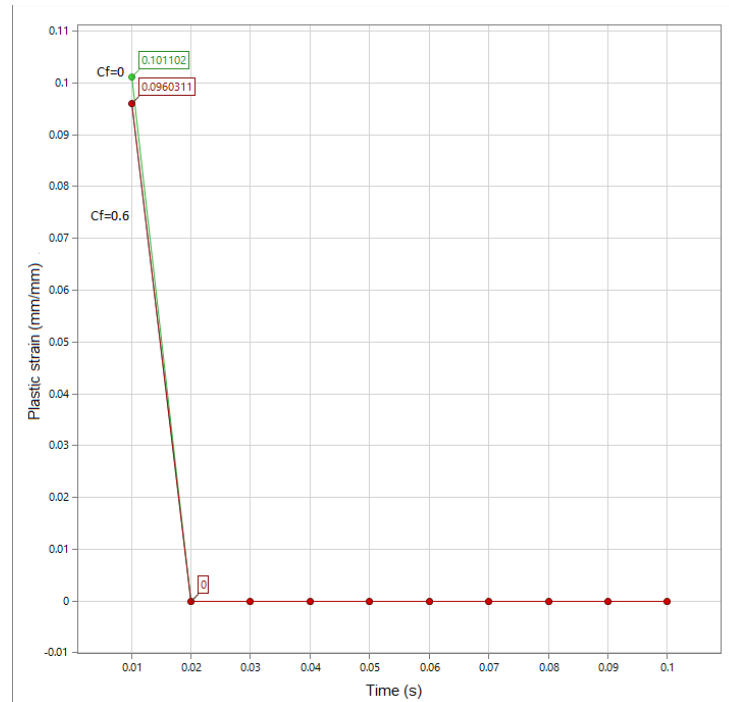
d) Von Mises stress variation on the board,  $\mu=0.6$

**Fig. 5.5** Variation of the plastic strain and Von Mises stress, for the impact on the structure at the frame C121 ( $x=64.62$  m,  $y=3.19$  m,  $z= 5.49$  m), with  $E= 400$  kJ ( $v=20$  m/s),  $T=100$  ms

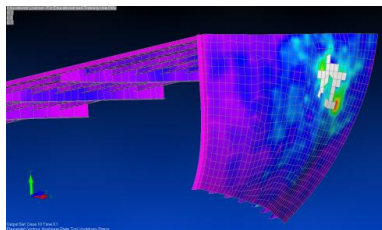
The labels a) of Fig. 5.5 and Fig.5.7 show variations of the plastic strain during the impact,  $T = 100$  ms, for the three values of the coefficient of friction,  $C_f$ , for the impact of the structure in the area of the frames C121 and C125, with the energy  $E = 400$  kJ.

Rupture behavior at the frame C121, illustrated in variants a) and d) of Fig. 5.5 shows a different behavior of the shell at the point of impact. The structure yields located near of the impact point, at the junction with the frame C121.

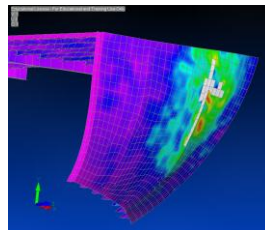
In label a) of Fig. 5.7 it is observed that the increase of the impact energy by 4 times leads to a failure of the shell, twice faster, along the frame C125.



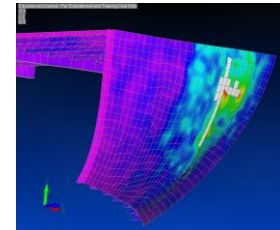
**a)** Variation of the plastic strain on the board for the element 4620



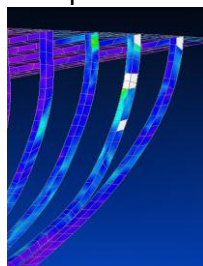
**b)** Von Mises stress variation on the board,  $\mu=0.0$



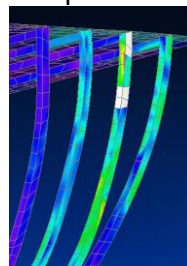
**c)** Von Mises stress variation on the board,  $\mu=0.4$



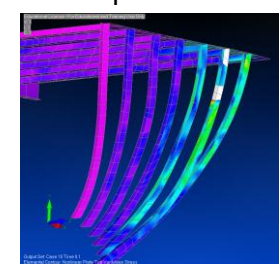
**d)** Von Mises stress variation on the board,  $\mu=0.6$



**e)** Von Mises stress variation on the frame,  $\mu=0.0$



**f)** Von Mises stress variation on the frame,  $\mu=0.4$



**g)** Von Mises stress variation on the frame,  $\mu=0.6$

**Fig. 5. 7** Variation of the plastic strain and Von Mises stress, for the impact on the structure at the frame C125 ( $x=66.62$  m,  $y=3.19$  m,  $z= 5.29$  m), with  $E= 400$  kJ ( $v=20$ m/s),  $T=100$  ms

In labels b), c) and d) of Fig.5.5 and Fig. 5.7 the possibility of breaking the shell is observed, with the visualization of the maximum length and width of the shell failure.

The yielding of the frame elements is a secondary problem, for the buoyancy of the hull, even if they fail before the shell.

In the labels e), f) and g) of Fig. 5.7 is observed, the influence of the coefficient of friction on the mode of rupture the structure, impacted with  $E = 400$  kJ ( $v = 20$  m / s), the surface affected



more being that of the variant e), without friction, where an extension of the effect on the frame C126 (1 broken element) is observed.

5.1.3 The analysis of the unmodified structure geometry's influence on the effects due to the impact depending on the friction coefficients between the elements of the structure and the impactor

In order to observe the behavior in time of the damage caused by the impact for different friction coefficients, it was necessary to analyze the variation of the Von Mises stresses for the structure of the impacted border in the C125 coastal area, for 2 times  $T = 70$  ms, respectively  $T = 100$  ms, from the beginning of the phenomenon. of impact. In the variants a), b) and c) of Fig. 5.8 the behavior on the shell can be observed at time  $T = 70$  ms. Similarly, in variants e), f) and g) of Fig. 5.8 the same behavior can be observed for  $T = 100$  ms. The numerical data are presented in Table 5.9.

**Table 5.9** The influence of friction on Von Mises stress variation during impact, at frame C125, with  $E=400$  kJ (20 m/s)

Time (ms)	Von Mises stress (MPa)		
	$\mu=0.0$	0.4	$\mu=0.6$
70	571	653	641
100	721	507	559

From the comparative analysis of the data in Table 5.9 and the diagrams in Fig.5.8, which show values of the variation of Von Mises stresses on the board, a different tendency is observed in case the friction is neglected compared to the one in which the friction is considered.

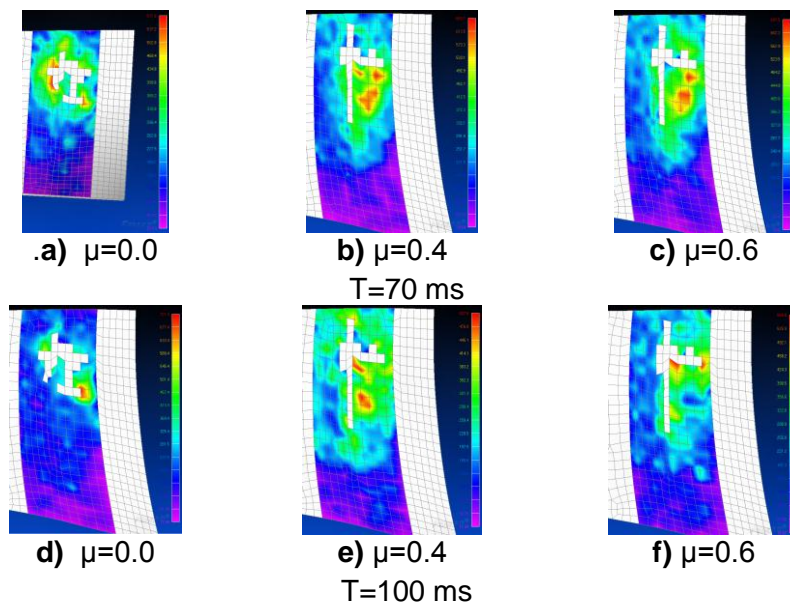


**Fig. 5.8** Diagrams of Von Mises stress variation on the board, for different friction coefficients, under impact loads at frame C125 ( $x=66.62$  m,  $y=3.19$  m,  $z= 5.29$  m), with  $E= 400$  kJ ( $v=20$ m/s)

Thus, at the end of the analysis, at  $T = 100$  ms, we observe a decrease in the variation of Von Mises stress with a maximum value of 29.68%, for the case of considering a friction

coefficient equal to 0.4, compared to the case of neglecting the friction. But at the time  $T = 70$  ms, the tendency is reversed. Thus, it is observed, at this moment, an increase in the variation of Von Mises stresses with a maximum value of 14.36% for the case of considering a friction coefficient equal to 0.4, compared to the case of neglecting the friction. The decreasing / increasing tendencies of the Von Mises stresses are similar, for both moments of time, if the comparative analysis is performed for the case of the coefficient of friction equal to 0.6 versus if the friction is neglected.

Similarly, the comparative analysis of the variation of Von Mises stress on the frame elements, impacted with the energy  $E = 400$  kJ (20 m / s) is performed. Thus, at the end of the analysis, at  $T = 100$  ms, we observe a decrease in the variation of Von Mises stresses with a value of 11.71%, for the case of considering a friction coefficient equal to 0.4, compared to the case of neglecting the friction. The trend is maintained for the moment  $T = 70$  ms, the decrease being with a value of 7.82%. The tendency to decrease the Von Mises stress is similarly for the time  $T = 70$  ms, when compared for the case of the friction coefficient equal to 0.6 versus the case where the friction is neglected. For the value of this coefficient of friction, at the end of the analysis at  $T = 100$  ms, we observe an increase of the variation of Von Mises stresses with a value of 1.18% for the case of considering a friction coefficient equal to 0.6, compared to the case of neglecting the friction.

Comparative analyzes for the study of the variation of Von Mises stresses for the impacted edge structure at the frame C125, for 2 times  $T = 70$  ms, respectively  $T = 100$  ms, from the beginning of the impact phenomenon, shows the nonlinear and complex aspect of the impact phenomenon.

From the analysis of the results of the numerical modeling, the influence of the geometry on the damaged area and volume is determined due to the impact with the two energies,  $E = 100$  kJ, respectively  $E = 400$  kJ.

The transition of the geometry from flat surfaces to curved surfaces, characteristic of the passage from the cylindrical area to the curved area, has an effect on both the damaged area and the destroyed volume.

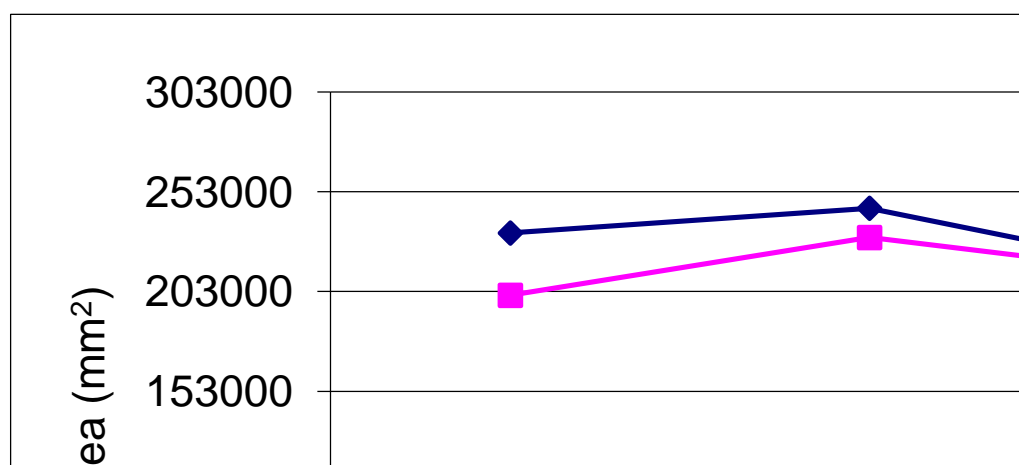


**Fig. 5.10.** Variation of the starboard's damaged area, impacted at frames C121, C123 and C125 (C study)

It is observed in the graph in Fig.5.10 that there is a tendency to increase the destructive effects from the frame C121 towards the bow, in the area of the frame C125, for  $E = 100$  kJ. It is observed that this tendency is opposite for  $E = 400$  kJ, these effects decreasing from the C121 frame towards the sample, for  $\mu = 0.6$ .

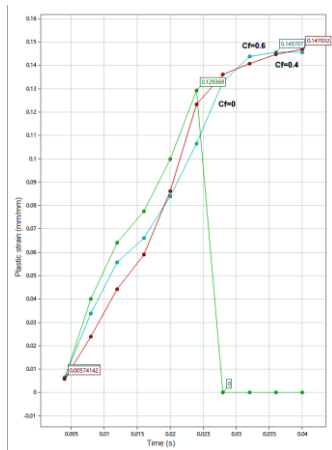
Thus, at the end, an increase with 96.56% for the volume and the damaged area is identified, at the impact of the shell near the frame C125 with  $E = 400$  kJ compared to the impact with  $E = 100$  kJ, considered at the end of the analysis.

The results obtained in the previous study had the role of clarifying, the specialized literature in the naval field providing little data in this regard, the impact behavior of the flat and curved naval structures. This subject, studied in §5.2, allows the approach of new geometries that lead to the reduction of the damaged areas, so that the integrity of the structure does not endanger the integrity of the entire ship.

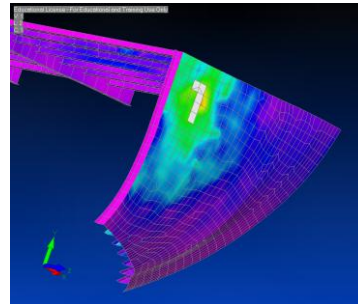
5.1.4. Study of the effects due to the impact loads at tensile tearing failure mode

Since from the first appearance of the shell it allows the water to enter the body or the release of toxic products for the environment, it is necessary to carry out a study in the first phases of the breaking process.

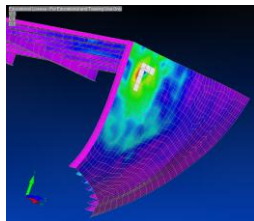
In the labels a) of Fig. 5.15 and Fig. 5.17 are shown diagrams of the plastic strain during the impact,  $T = 40$  ms, for the three values of the coefficient of friction,  $C_f$ , for the impact of the structure at frames C121 and C125, with the energy  $E = 144$  kJ. The zero value of this parameter marks the breakdown of the respective element. The plastic strain of the shell is observed at the frame C121, illustrated in label a) of Fig.5.15. The increase of the impact energy by 44% determines the increase of the damaged area on the shell by 202%, in case the friction is neglected, and by 140% for  $\mu = 0.4$ . The rupture of the impacted shell in the C125 coastal area, can be visualized, for all values of  $\mu$ , in labels a), b), c) and d) of Fig. 5.17.



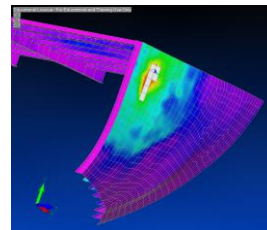
a) Variation of the plastic strain on the board for the element 4807



b) Von Mises stress variation on the board,  $\mu=0.0$



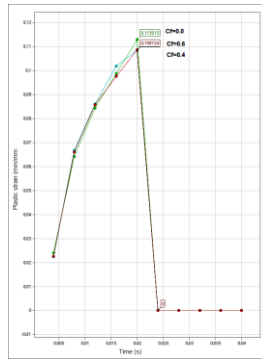
c) Von Mises stress variation on the board,  $\mu=0.4$



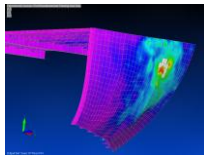
d) Von Mises stress variation on the board,  $\mu=0.6$

**Fig. 5.15** Variation of the plastic strain and Von Mises stress, for the impact on the structure at the frame C121 ( $x=64.62$  m,  $y=3.19$  m,  $z= 5.49$  m), with  $E= 144$  kJ ( $v=12$  m/s),  $T=40$  ms

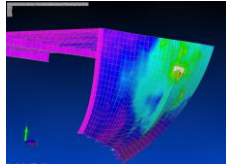




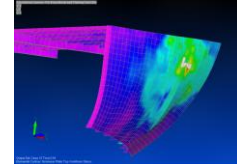
a) Variation of the plastic strain on the board for the element 4620



b) Von Mises stress variation on the board,  $\mu=0.0$



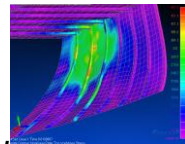
c) Von Mises stress variation on the board,  $\mu=0.4$



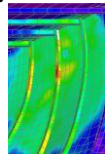
d) Von Mises stress variation on the board,  $\mu=0.6$

**Fig. 5.17** Variation of the plastic strain and Von Mises stress, for the impact on the structure at the frame C125 ( $x=66.62$  m,  $y=3.19$  m,  $z= 5.29$  m), with  $E= 144$  kJ ( $v=12$  m/s),  $T=40$  ms

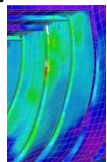
Fig.5.18 shows the process of occurrence of the structure breakdown for 4 moments of time, until the moment  $T = 40$  ms. In the labels a), b), c) and d) of Fig. 5.18, the yielding of the impacted structure at the frame C125 with the energy  $E = 100$  kJ ( $v = 10$  m / s) is illustrated. Similarly, in labels e), f), g) and h) of Fig. 5.18 the same process is observed for impacting the structure with  $E = 144$  kJ ( $12$  m / s).



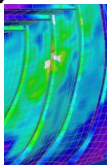
a)  $T=10$  ms



b)  $T=20$  ms

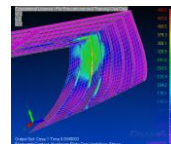


c)  $T=30$  ms

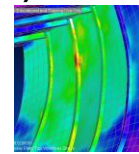


d)  $T=40$  ms

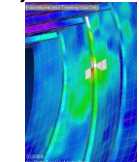
$E= 100$  kJ ( $v=10$ m/s)



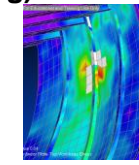
e)  $T=10$  ms



f)  $T=20$  ms



g)  $T=30$  ms



h)  $T=40$  ms

$E= 144$  kJ ( $v=12$  m/s)

**Fig. 5.18.** Structure's rupture under impact loads at frame C125 ( $x=66.62$  m,  $y=3.19$  m,  $z= 5.29$  m),  $\mu=0$

It is observed that the rupture process intensifies after the time  $T = 20$  ms, so that at the time  $T = 30$  ms, it is observed that an increase of 44% of the impact energy causes an increase of the damaged area by 85%, with the failure of the board. The phenomenon is presented in labels c) and g) of Fig. 5.18. Since between the moment  $T = 20$  ms and  $T = 30$  ms there are 10,000 steps of the analysis that have not been illustrated. It is possible to identify the moment when the structure break is similar, for the two energy values, at different times. Knowing the extent of the damage caused by the impact of two naval structures, damages that can lead to loss of buoyancy and / or environmental pollution, rules regarding the speed of navigation can be given for each type of ship, so that possible accidents are not with major consequences

In order to study the influence of the geometry on the rupture, 18 collision scenarios were performed, and analyzing in comparison, the variation of the Von Mises stresses for impacting the structure with the two values of energies, both in the case of the existence of friction with a value of 0.4, and in the absence of friction, it is observed that an increase of 44% of the impact energy causes an increase of the variations of the Von Mises stress, at the moment  $T = 40$  ms, with 32.05% for the case of neglecting the friction, and with 38.64%, for an impact with a coefficient of friction between the hull and impactor equal to 0.4.

## 5. 2. Design solutions to reduce collision effects

In order to diminish the effects of the collision on the naval structure, the observations of paragraph 5.1 are used, being proposed two design options through which modifications to the geometric characteristics and curvature of the naval structure will be presented, in §5.2.1, respectively in §5.2.2.

### 5.2.1. Redesign of the geometrical characteristics of the structure (the shell's and frame 's element thickness's modification)

You can choose solutions, modify the thickness tables, at the frame C125, according to the variant presented in Table 4.10 of chapter 4 (see §4.3).

The diagrams in Fig. 5.21 and Fig. 5.22 illustrate the behavior of the impacted framing structure in the C125 frame area with energies  $E = 100$  kJ (10 m / s) and  $E = 400$  kJ (20 m / s), for three values of the friction coefficient.

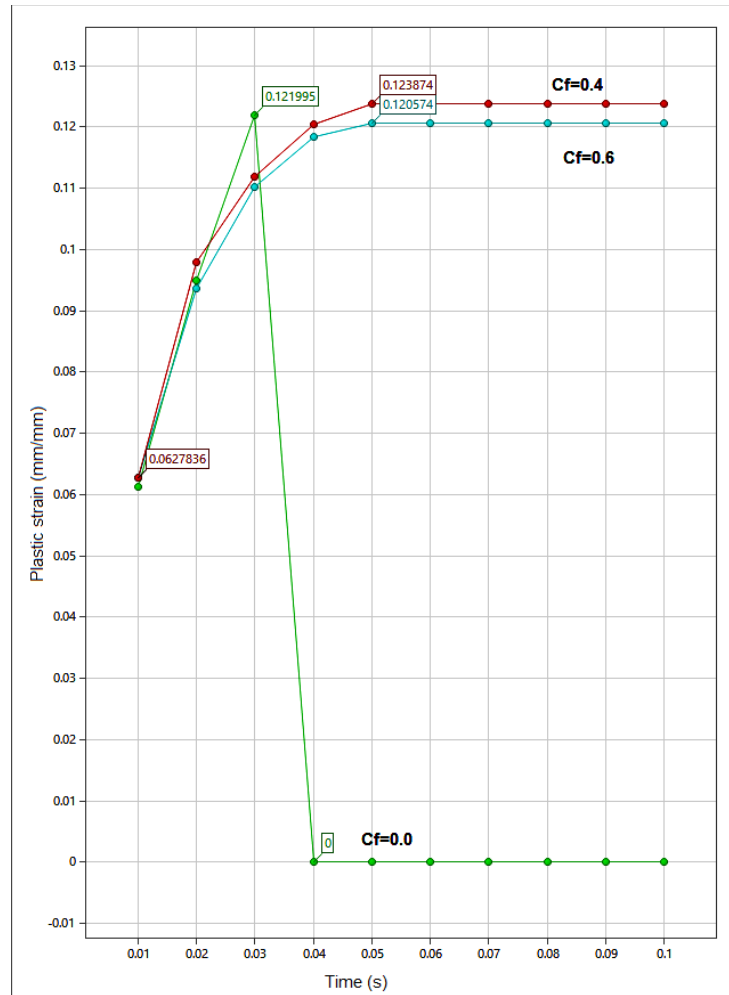
In the label a) of Fig. 5.21 is shown the diagram of the plastic strain during the impact,  $T = 100$  ms, for the three values of the coefficient of friction,  $C_f$ , for the impact of the structure in the area of the frame C125, with the energy  $E = 100$  kJ. The zero value of this parameter marks the break of the respective element.

It is observed, from labels b), c) and d) of Fig. 5.21, the variation of the Von Mises stresses on the impacted shell at the C125 frame area, for variant II of redesign. Thus the damaged area of the redesigned casing, by increasing the thickness of the sheet (variant II), decreases by 75% compared to the similar values of the unmodified structure, for  $\mu = 0.0$ .

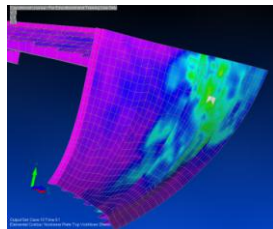
In the variant of redesigning the structure, by increasing the thickness of the sheet (variant I), the damaged area is identical to the initial one. In the labels e), f) and g) of Fig. 5.21 are presented the variations of the Von Mises stresses on the impacted structure at the C125 frame area, for variant II of redesign.

There are no major differences regarding the damaged areas on the structure.

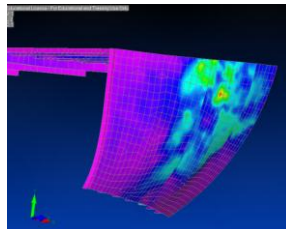
In the label a) of Fig.5.22, the variation of the specific plastic strain for the impact of the structure at the C125 frame area is presented, with the energy  $E = 400$  kJ ( $v = 20$  m / s). The breakdown of the structure in the impact area is observed, yielding both the frame and the shell.



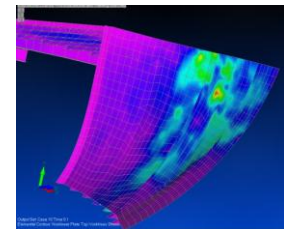
a) Variation of the plastic strain on the board for the element 4620



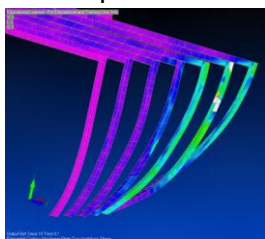
b) Von Mises stress variation on the board,  $\mu=0.0$



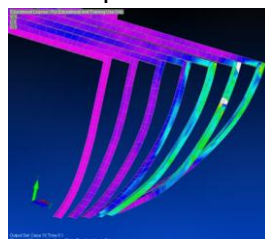
c) Von Mises stress variation on the board,  $\mu=0.4$



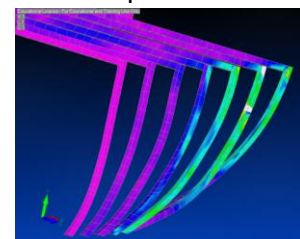
d) Von Mises stress variation on the board,  $\mu=0.6$



e) Von Mises stress variation on the frame,  $\mu=0.0$



f) Von Mises stress variation on the frame,  $\mu=0.4$



g) Von Mises stress variation on the frame,  $\mu=0.6$

Fig. 5.21 Variation of the plastic strain and Von Mises stress, for the impact on the redesign board at the frame C125 ( $x=66.62$  m,  $y=3.19$  m,  $z= 5.29$  m),  $cu E= 100$  kJ ( $v=10$  m/s),  $T=100$  ms (Variant II)

In the labels b), c), d), e) and f) of Fig. 22, the impact behavior of the redesigned structure (variant I) is observed, depending on the three values of the friction coefficient. We observe a decrease of the damaged area on the frame by 29.65% of the variant I, in which the thickness of the frame was changed, compared to the unmodified structure, for  $\mu = 0.6$ .

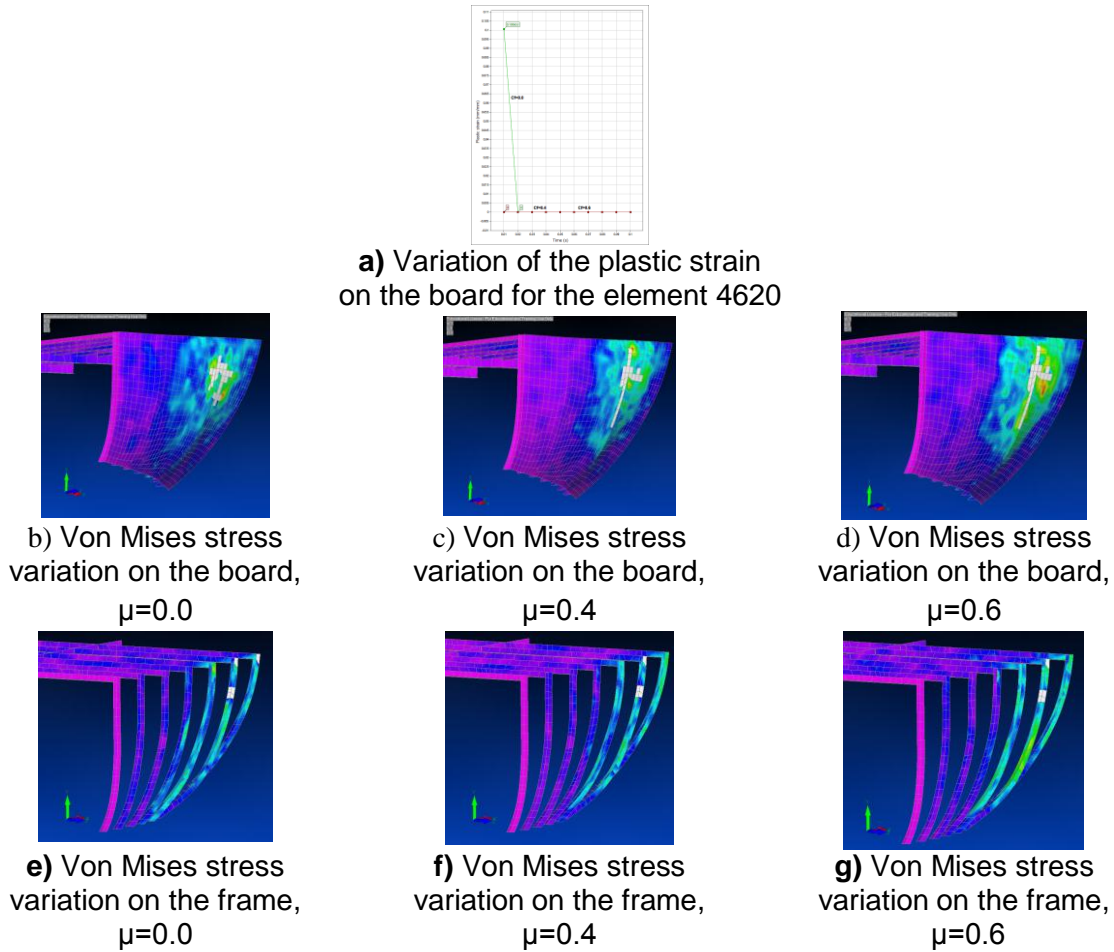


**Fig. 5.22** Variation of the plastic strain and Von Mises stress, for the impact on the board at the redesigned frame C125 ( $x=66.62$  m,  $y=3.19$  m,  $z= 5.29$  m), with  $E= 400$  kJ ( $v=20$  m/s),  $T=100$  ms (Variant I)

In order to study the influence of the new geometry on the rupture, 12 collision scenarios were realized. In Fig.5.24 is presented the comparative analysis of the variation of the damaged areas depending on the friction coefficients, for the redesigned and the unmodified structures, at the impact with  $E = 100$  kJ ( $v = 10$  m / s).

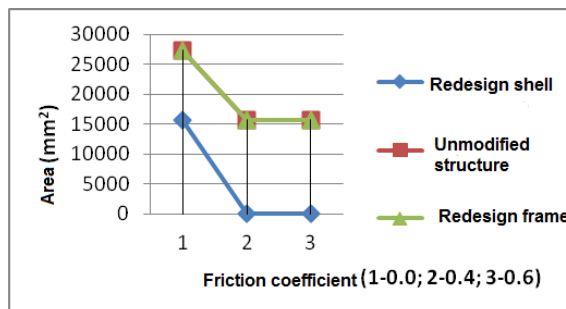


**Fig. 5.24** Variation of the starboard's damaged area, impacted at frame C125, with  $E=100$  kJ ( $v=10$  m/s), for initial and redesigned structure, depends on different friction coefficients

We observe the lack of damage on variant II, for  $\mu = 0.4$  and  $\mu = 0.6$ , at which the thickness of the shell board was changed.

From the graph presented in Fig.5.25, we observe a better behavior of the structure compared to the initial geometry, for the C125 frame redesign variant (variant I), for  $\mu = 0.6$ , which determines the decrease with 29.65% and 1.67% of the area, respectively volume of the damaged area, impacted by  $E = 400$  kJ ( $v = 20$  m / s).

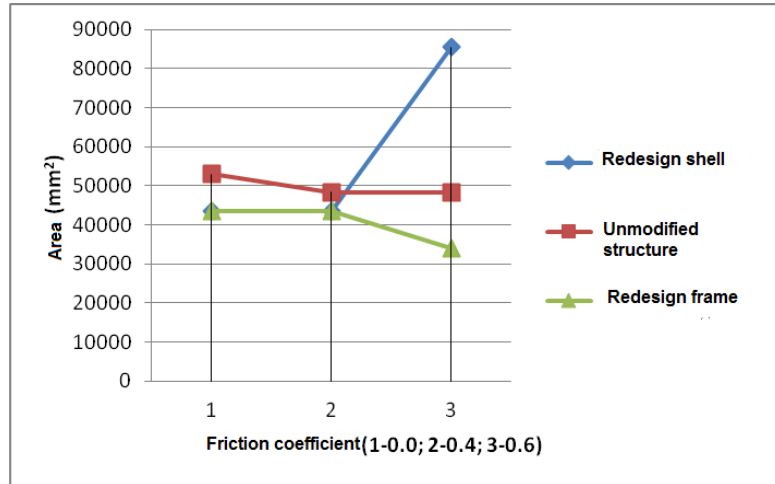


**Fig. 5.25** Variation of the frame's damaged area, impacted at frame C125, with  $E=400$  kJ ( $v=20$  m/s), for initial and redesigned structure, depends on different friction coefficients

### 5.2.2. Redesign the curvature of the frame

The structure at frame C125 was modified by moving 6 points (Variant III), towards the interior of the ship along the Z direction, symmetrically on both sides. The initial position of the points is presented in Table 5.21 and their displacement, after transformation, is mentioned in Table 5.22.

**Table 5.21** Points's position of initial structure, at C125, starboard

Position from Fig. 5.26	Coordinate (mm)			Node (Tb.)
	X	Y	Z	
6	66625	1796	4409	3641
1	66625	1951	4593	3639
3	66625	2060	4698	3638
4	66625	2146	4769	3637
5	66625	1830	4454	5981
2	66625	1871	4503	3640
S	66625	1726	4311	3642
T	66625	2237	4828	3636

The positioning of the points on the starboard, at frame C125 is shown on the curves and on the mesh elements illustrated in Fig. 5.26, the nodes S and T being fixed. The modifications made do not affect the surface of the shell, which has, in the end, a single curvature.

**Table 5.22** The change of the frame's curvature along the Z axis at C125 (x=66.62 m, y=3.19 m, z= 5.29 m), starboard (Variant III)

Geometry	Distance (mm)					
	1	2	3	4	5	6
Model 1	-7	-7	-5	-5	-5	-5
Model 2	-11	-11	-7	-7	-7	-7
Model 3	7	7	5	5	5	5
Model 4	11	11	7	7	7	7

For the new geometries, the quality of the mesh elements was evaluated [67]. The obtained Jacobian value is 0.6 for the four models, being very close to the Jacobian value of the initial geometry (J = 0.597).

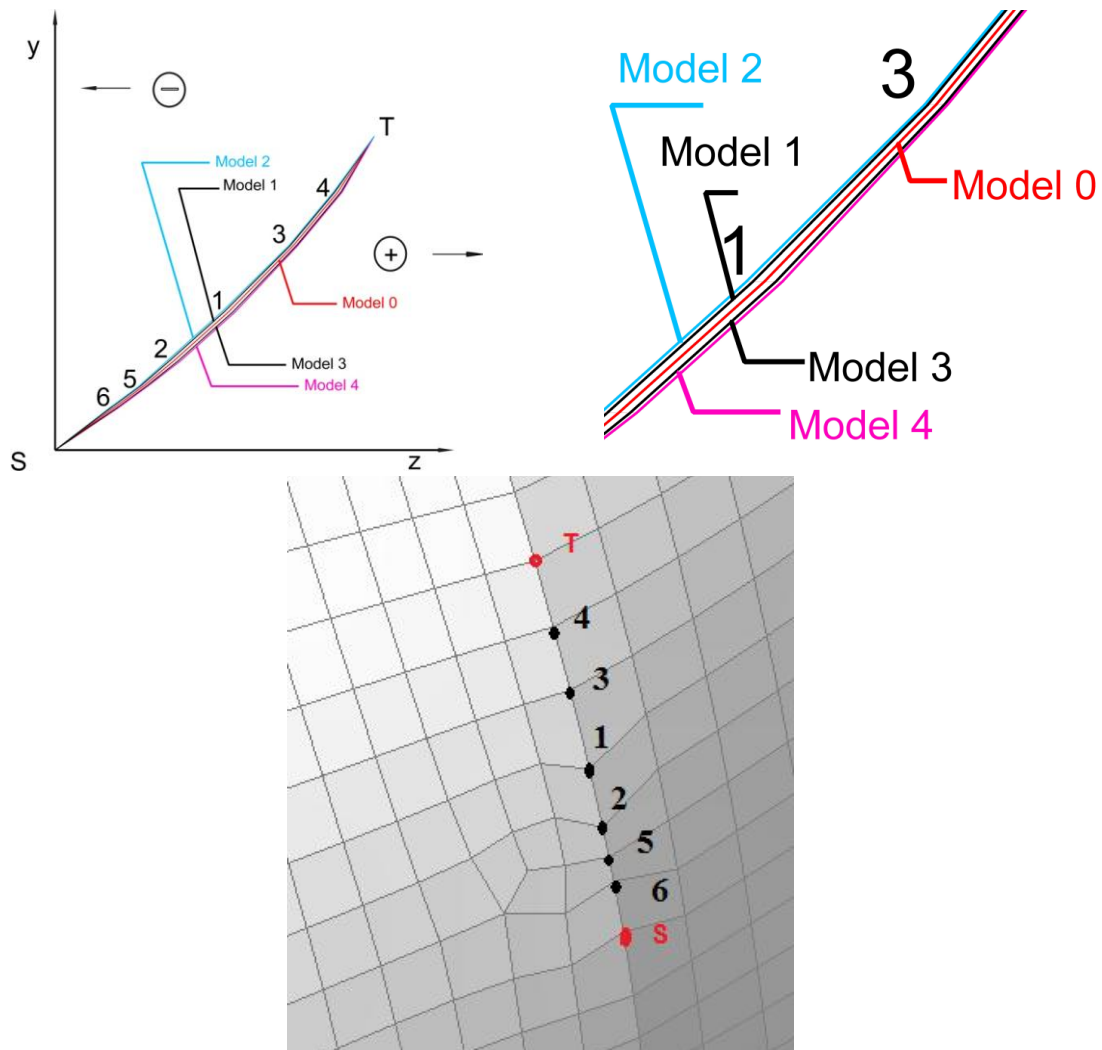
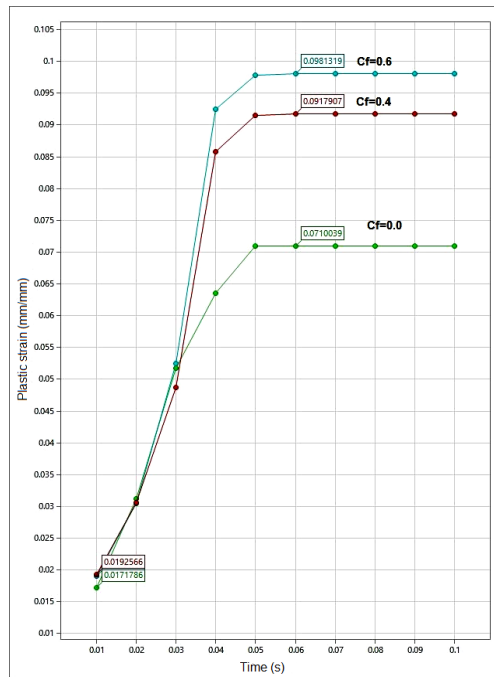


**Fig. 5.26** Curvature's structure changing at frame C125, start from initial structure (initial model), M0, to new models M1, M2, M3 and M4

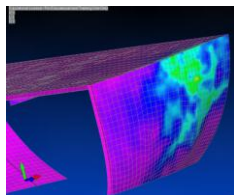
The Free Edges option in the MeshToolbox menu allowed the contact to be evaluated in the structure modification area. The visualizations carried out showed that no detachments appeared after the transformations made. In order to study the behavior of the new impact geometries, another 24 collision scenarios (6 for each model) were performed.

Similar data were obtained from the numerical analysis data for models 1 and 2.

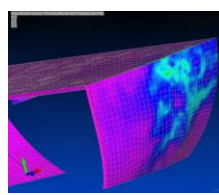




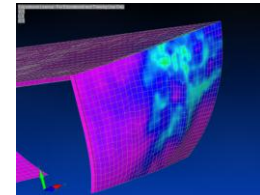
a) Variation of the plastic strain on the board for the element 4620



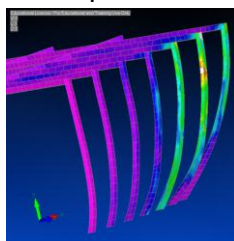
b) Von Mises stress variation on the board,  $\mu=0.0$



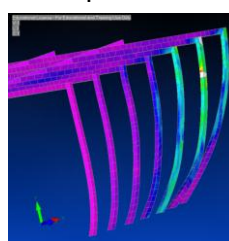
c) Von Mises stress variation on the board,  $\mu=0.4$



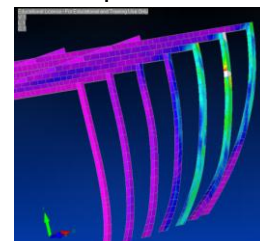
d) Von Mises stress variation on the board,  $\mu=0.6$



e) Von Mises stress variation on the frame,  $\mu=0.0$



f) Von Mises stress variation on the frame,  $\mu=0.4$



g) Von Mises stress variation on the frame,  $\mu=0.6$

**Fig. 5.30** Variation of the plastic strain and Von Mises stress of the structure with the redesigned curvature, impacted at the frame C125 ( $x=66.62$  m,  $y=3.19$  m,  $z= 5.29$  m), with  $E= 100$  kJ ( $v=10$  m/s),  $T=100$  ms (Variant III, model 3)

In the label a) of Fig. 5.30 is presented the diagram of the plastic strain at the end of the impact,  $T = 100$  ms, for the three values of the coefficient of friction,  $C_f$ , for the impact of the structure in the area of the C125 frame, with the energy  $E = 100$  kJ, for the models 3. An increase is observed on the plastic strain, with a value of 21.97% for the case where the influence of the friction with  $\mu = 0$  is considered, compared to the case where the friction is neglected. The contact between the elements of the barge-impactor assembly, evidenced by the friction coefficients, causes an increase of the variation of the plastic strain by 0.06, of the friction coefficient  $\mu = 0.6$  compared to  $\mu = 0.4$ . As a result of the impact, the shell remains deformed in the plastic field without entering the breaking stage. This effect is observed also in

the labels b), c) and d) of Fig. 5.30, where the variation of the Von Mises stresses on the impacted shell at the frame C125 is presented, for the 3 redesign model.

The labels e), f), g) and h) of Fig. 5.30 show the variation of Von Mises stress on the impacted frame with the same energy. There is a decrease of the variation of the damaged areas with a value of 26.79%, for the case of the curvature modification according to model 3 (see Fig. 5.26) compared to the unmodified structure, only for  $\mu = 0.0$ . There are no modifications of the redesigned frame damage to the unmodified structure, in cases where the influence of friction is considered.

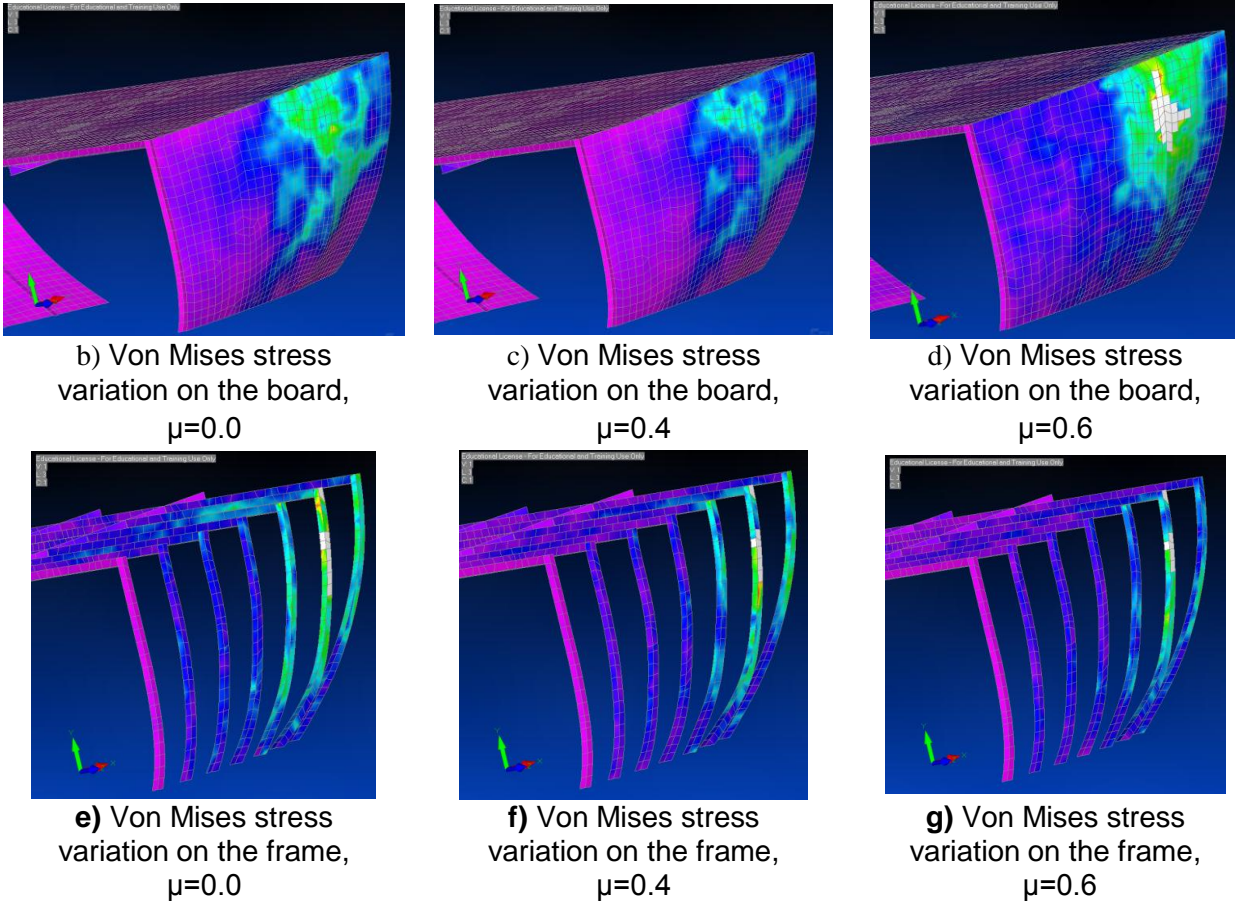


**Fig. 5.34** Variation of the plastic strain and Von Mises stress of the structure with the redesigned curvature, impacted at the frame C125 ( $x=66.62$  m,  $y=3.19$  m,  $z= 5.29$  m), with  $E= 400$  kJ ( $v=20$  m/s),  $T=100$  ms (Variant III, model 3)

### 5.2.3 Evaluation the influence of frame's curvature on the effects due to the impact loads

The analysis of the data determines the influence of the curvature of the structure on the area and the volume damaged due to the impact with the energy  $E = 100$  kJ ( $v = 10$  m / s), for four models. It can be observed that both the damaged areas and volumes have the same growth or decrease trends compared to the similar values of the initial geometry, as a percentage having identical values for all new models. A decrease of 42.84% of the damaged area on the shell is identified only for  $\mu = 0$  compared to the initial geometry, while the damaged area on the frame is unchanged, for the first two new models. For the other values of the coefficient of friction no changes are observed. For model 3 and model 4, a decrease of 26.79% of the damaged area on the frame is observed only for  $\mu = 0$ . In these models, on the shell, the damage is zero. It can be observed that the modification of the curvature of the frame in the model 2 compared to the model 1 did not generate changes of the effects due to the impact, both for the shell and for the frame.



Similarly, the influence of the structure's curvature on the area and the damaged volume is determined, due to the impact with energy  $E = 400 \text{ kJ}$ , for the four models.

The damaged areas and volumes of the four modified structures were compared with the similar values of the unmodified geometry. We observe a tendency to increase the variation of the damage on the shell with a maximum value of 52%, for  $\mu = 0.6$ , for models 1 and 2 compared to the initial geometry, as can be seen in the graph in Fig.5.36. For models 3 and 4, there is a tendency to decrease the variation of the damage on the shell, with a maximum value of 11.54%, for model 3 with respect to the initial geometry, for  $\mu = 0.6$ .

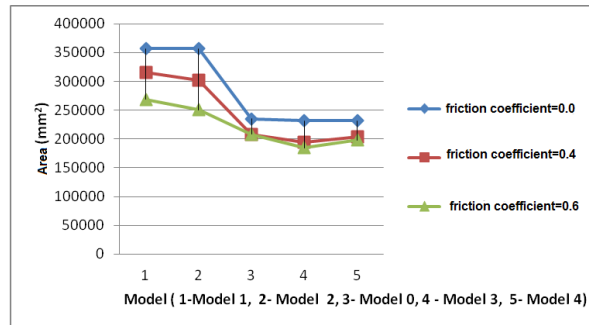


**Fig. 5.36** The influence of friction coefficient on the damage's area on starboard for four models, impacted at the frame C125 with  $E=400 \text{ kJ}$  ( $v=20\text{m/s}$ )

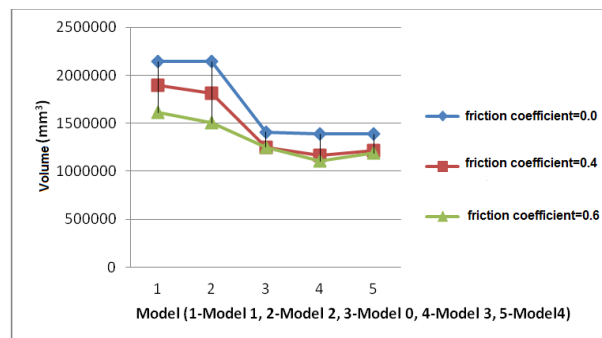


**Fig. 5.37** The influence of friction coefficient on the damage's volume on starboard for four models, impacted at the frame C125 with  $E=400 \text{ kJ}$  ( $v=20\text{m/s}$ )

In Fig. 5.37 are presented the variations of the damaged volume of the impacted shell at the C125 frame area with the same energy depending on the friction coefficient. We observe a tendency similar to that of the variation of the damaged areas, shown in Fig.5.36.

The decrease of the variation of the damage on the frame is registered only for model 3, having the value 2.87, for  $\mu = 0.6$ .

It is known that the safety of ships is given by the integrity of their board shell. Thus, it was considered necessary to analyze the variation of the Von Mises stresses for the board shell of the model 3 (see Fig.5.26), impacted with  $E = 400 \text{ kJ}$  ( $v = 20 \text{ m / s}$ ), at the area of the C125 frame. The process of rupture occurrence was studied for 5 time points, up to the time  $T = 50 \text{ ms}$  from the beginning of the collision. The numerical data resulting from the analysis of model 3 are compared with similar data for the initial, unmodified geometry.

In Fig.5.38 and Fig.5.39 is shown the variation of the Von Mises stresses for the impacted coating, with the energy  $E = 400 \text{ KJ}$  ( $v = 20 \text{ m / s}$ ), for  $\mu = 0.4$ , at the C125 frame area. The structure's behaviour of initial model (model 0) is seen in labels a), b), c), d) and e) of Fig.5.39, and in labels f), g), h), i) and j) of Fig.5.39 is observed the same information for model

3. It is identified, from the graph in Fig.5.38, that until  $T = 20$  ms, the Von Mises voltages of the two models have reduced differences between them (4.5%).

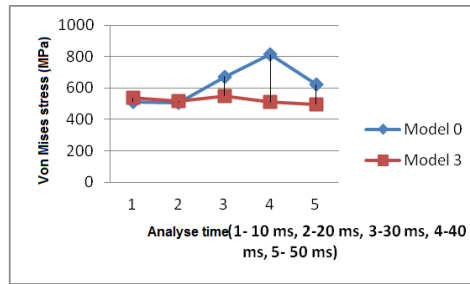


**Fig. 5.38.** Von Mises stress variation on the board, impacted at the frame C125, with  $E=400$  kJ ( $v=20$  ms),  $\mu=0.4$ , Initial model model 0 and model 3

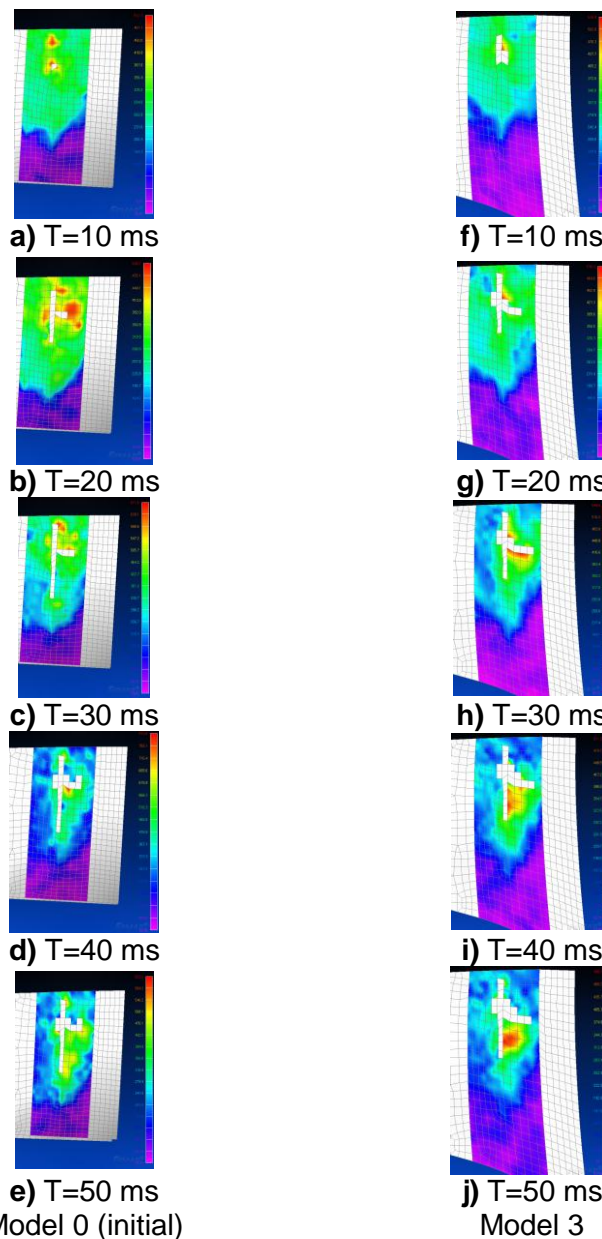


**Fig. 5.39** Diagrams of Von Mises stress variation on the board under impact loads at frame C125 ( $x=66.62$  m,  $y=3.19$  m,  $z= 5.29$  m),  $\mu=0.4$

At the time  $T = 40$  ms, the maximum decrease of the Von Mises stress variation with a value of 37.22% is identified, for the model 3 compared to the model 0 (initial). Thus, it is possible to justify the reduction of the damage that appears at the end of the analysis, on the shell, by 11.54%, reduction due to the modification of the geometry according to Fig. 5.26. Considering that the results obtained for model 4 do not respect the same tendency of the damages for the impacted structure, it can be concluded that the curvature modification is only performed locally, in the vicinity of the initial geometry.

In the graph in Fig. 5.40, one clearly observes the dependence of the variation of the structure geometry damage on the impact velocity. Thus, when impacting the structure of the boarding with the speed  $v = 10$  m / s, there are no visible changes of the damage for the 4 redesigned models, according to Fig. 26, compared to the initial structure, unchanged. When impacting the structure with  $v = 20$  m / s, we observe a varied behavior of the redesigned models with respect to the unmodified structure. Thus, from the graph in Fig.5.40 it can be quickly identified that model 3 is the one with the best impact behavior, from the proposed ones.

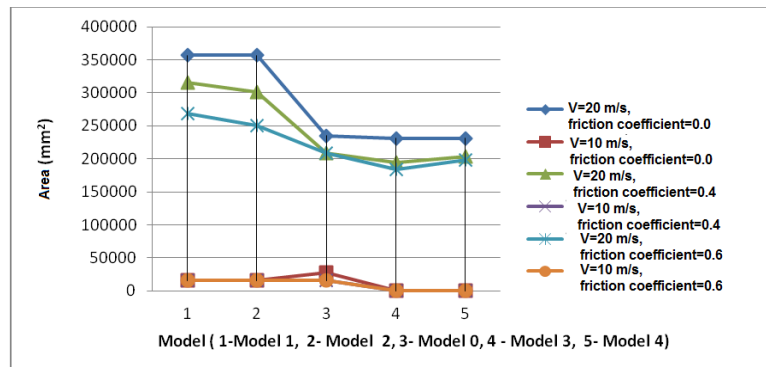


**Fig. 5.40** The influence of geometry on damage area of the shell impacted at C125 frame depending on the friction coefficients, for 4 redesign models

### 5.3. Concluding remarks

The following conclusions were drawn from analysing the 72 scenarios of this chapter, considering the influence the velocity and the friction coefficient:

1. The effects are local for all the variants of the ship's structure side collision, the frames yielding faster than the board, which ensures the buoyancy of the ship for a period of time.
2. The increase of the impact energy of 4 times determines the half of the time of the starboard failure.
3. Increase by 96.56% of the volume and area of the damaged surface when impacting the starboard near the C125 frame for the impact with  $v = 20$  m / s ( $E = 400$  kJ) compared to the impact with  $v = 10$  m / s ( $E = 100$  kJ).
4. The increase in table thickness of the starboard shell with 16.6% causes an increase of the structure's mass by 5.42% and the hardening of the starboard, so that at an the impact velocity with  $v = 10$  m / s ( $E = 100$  kJ) it does not fail, unlike the initial geometry where the board is broken (variant II).
5. The increase in table thickness of the frames with 16.6% causes an increase of the structure's mass by 2.3 % and the decrease with 29.65% of the area and 1.67% of the volume of the damaged frames, collided with  $v = 20$  m / s ( $E = 400$  kJ), for  $\mu = 0.4$ , compared to similar values of the initial geometry (variant I).

6. The modification of the frame's curvature causes an decrease of the damage compared to the initial geometry, with maximum relative variation's values of 11.54% for the board, and 2.87% for the damages of the frame at  $\mu = 0.6$ , at the impact with the energy  $E = 400$  kJ ( $v=20$  m/s) (variant III).

7. The modification of the frame's curvature, when double the impact speed for model 3, causes a decrease with 2.87%, compared to initial model,  $\mu = 0.6$ .

In the numerical analyzes performed in this chapter it was observed that the changes of the geometrical characteristics of the structure directly influence the length of the damaged area, at the impact with the energy  $v = 10$  m / s ( $E = 100$  kJ) that determines the reaching of the plastic stage, as opposed to the impact with the energy with  $v = 20$  m/s ( $E = 400$  kJ), that causes the reaching of the rupture stage when the value of the damaged area becomes dependent on the structure's curvature, the model 3 having the best behaviour under impact loads compared to initial structure.

## CHAPTER 6

### FINAL CONCLUSIONS. PERSONAL CONTRIBUTIONS. FUTURE RESEARCH PERSPECTIVES.

#### 6.1. Final conclusions

The naval structures, in particular the barges designed at ICEPRONAV-Galati, up to 1989, respond to the recommendations of the rules of resistance in the elastic field. As traffic on the Danube in recent years has increased and many of Romanian ships are used, it becomes necessary to analyze their structure in plastic field in order to improve ship safety and the risk of inland environmental pollution. In the naval field, the impact phenomenon is regulated by the norms included in DNV GL-RP-204 issued in 2017, which standardizes the design that ensures the safety of the ships operations, in case of accidental loads on their structure.

The numerical analysis using the finite element method is efficient for studying the behavior of the impacted naval structures, taking into account the rules of DNV-GL-RP-C208. The norms refer mainly to the discretization of the structure in finite elements, the application of the boundary conditions, the behavior of the non-linear material and the yield criteria.

The determination of the calculation methodology for studying the behavior of the structure of the bow area, for the 2000TDW barge, was performed on the basis of experimental tests. Following the impact of two models with a steel spherical mass, their elastic-plastic deformation was found. The two models used are:

- Experiment 1 - metal surface (steel S235) having a radius of radius  $R = 213.75$  mm;
- Experiment 2 - metal surface (steel S235) having a radius of radius  $R = 226.59$  mm.

Model's displacements were determined (in the direction of application of the force) and the contact force between the steel table and the shell surface of the model. The comparative analysis between the experimental results and those of the corresponding numerical simulations is illustrated, as a percentage, in Table 6.1:

**Table 6.1.** Comparative centralizer  
experiment - numerical simulations

Nr.	Experiment	Differences (%)		
		Displacements (simulation vs. experiment)	Displacements (curvature 2 vs. curvature 1)	
			Experimental	Simulation
1	Experiment 1	- 4.39	-	
2	Experiment 2	8.05	-15.76	- 4.80

The maximum difference for the displacement of the node in the impacted area, between experiments and numerical simulations is 8.05%, a value included in an acceptable range used in the field of naval structures (5-10%). It can be observed that the model in experiment 2, characterized by a smaller curvature, determines both experimentally and numerically the decrease of the effects at the point of impact.

The proposed numerical analysis method for the model of the material, necessary in studying the structure, and verified on the basis of the experimental tests, is used as a preliminary to analyze the behavior at the impact of the main deck of the 2000T barge test and then at the side impact of the same structure. The numerical model of the naval structure used

in the comparative analysis is built according to the rules DNV-GL-RP-C208 and DNVGL-CG-0127.

From the analysis of the data obtained from the numerical simulation of the impact of the naval structure, the following results were obtained:

- it can be determined to reach the plastic deformation stage of the structure under impact loads by analyzing the plastic deformation (see §3.2);
- it is recommended to consider the coefficient of friction for the realistic failure of the structure (see §3.3 and §4.1);
- design variants of the structure's geometrical characteristics can be identified to reduce the stresses under impact loads, by analyzing the local behavior of the structural elements, to reach the plastic stage (see §4.2. and §4.3);
- it is possible to determine the reaching of the structure's rupture stage under impact loads, by analyzing the plastic deformation (see §5.1);
- design variants of the structure's geometrical characteristics and modifying the curvature of the frame can be identified to reduce the stresses under impact loads, by analyzing the local behavior of the structural elements, to reach the rupture stage (see §5.2)

After analyzing the deformation and yielding modes of the frame and the board's structure, under impact loads, the following investigation variants were identified:

- dimensioning of the frame in the affected area for increasing the resistance (variant I) at the impact with the energy  $E = 100 \text{ kJ}$  ( $v = 10 \text{ m/s}$ ) (variant I,  $E=100 \text{ kJ}$ ,  $v=10 \text{ m/s}$ );
- sizing the board's shell in the affected area for increasing the resistance (variant II) at the impact energy  $E = 100 \text{ kJ}$  ( $v = 10 \text{ m/s}$ ) (variant II,  $E=100 \text{ kJ}$ ,  $v=10 \text{ m/s}$ );
- sizing of the frame in the affected area to reduce the effects of the impact (variant I) with the energy  $E = 400 \text{ kJ}$  ( $v = 20 \text{ m/s}$ ) (variant I,  $E=400 \text{ kJ}$ ,  $v=20 \text{ m/s}$ );
- dimensioning of the board's shell in the affected area to diminish the effects of the impact (variant II) with the energy  $E = 400 \text{ kJ}$  ( $v = 20 \text{ m/s}$ ) (variant II,  $E=400 \text{ kJ}$ ,  $v=20 \text{ m/s}$ );
- changing frame's curvature shall for diminishing the response to impact (variant III) with energy  $E = 100 \text{ kJ}$  ( $v = 10 \text{ m/s}$ ) and  $E = 400 \text{ kJ}$  ( $v = 20 \text{ m/s}$ ) (variant III,  $E=100 \text{ kJ}$ ,  $v=10 \text{ m/s}$  și  $E=400 \text{ kJ}$ ,  $v=20 \text{ m/s}$ ).

After analyzing the geometries modification of the structure described above, it can be concluded:

- a method of diminishing the Von Mises stresses of the board is to increase the thickness of the shell, in the area with greater curvature, for the impact variants that have generated the plastic stage;
- a method of diminishing the damaged area is the increase of the thickness of the frames for the variants in which the impact energies generated the rupture stage.

Considering the two main objectives set: the decreasing of stress in the structure and the diminishing of the damaged area as a result of the impact, it was observed that the new structures met the proposed objectives as follows:

- Von Mises stresses reduction of 3.47% of the structure compared to the similar values of the initial geometry, for the variant in which the energies generated the plastic stage, for the dimensioning variant of the geometrical characteristics of the structure (variant I, E=100 kJ, v=10 m/s);
- cancellation of the effects of the impact in the damaged area on the board, for the variants in which the energies generated the plastic stage, for the variant of sizing the geometrical characteristics of the structure (variant II, E=100 kJ, v=10 m/s);
- the reduction by 29.65% of the area and by 1.67% of the volume of the damaged structure, for the variants in which the energies generated the rupture stage, compared to similar values of the initial geometry, for the variant of sizing the geometrical characteristics of the structure (variant II, E=400 kJ, v=20 m/s)
- the decrease of the damaged area on the board, by modifying the structure's curvature, by 11.54% only for  $\mu=0.6$ , compared to initial structure (variant III, E=100 kJ, v=10 m/s);

From this study we can draw the following synthetic conclusions:

- a) Vessels are designed today, by studying elastic behavior. The response is studied in the field of plastic accidental situations only provided for classification societies (DNVGL-RP-204).
- b) The numerical analysis based on the Finite Element Method allows the investigation of the design solutions of the ship geometry for improving the behavior of the structures at impact.
- c) Six structural naval models (variant I, variant II and 4 for variant III) have been designed that correspond to the imposed objectives (diminishing the tensions in the structure and diminishing the damaged area following the impact), using the numerical analysis based on the Finite Element Method for the behavior in the plastic field.

## 6.2. Personal contributions

The purpose of the research activities carried out within this thesis was to design a procedure for modifying the structure of the 2000TDW barge's bow area, which would meet the requirements for increasing the operational safety.

Achieving the goal mentioned above is based on original contributions following:

- 1) Validation of the calculation methodology, by choosing a material model, experimentally verified by numerical simulation in chapter 2, the maximum difference for displacement being included in an acceptable range used in the field of naval structures.
- 2) Analysis of the various effects produced by the impact of the barge in various scenarios of speed and kinetic energy of impact. Establishing the input parameters, for numerical analysis based on the Finite Element Method in the calculation of the bow's barge structure, based on the experimental data.
- 3) The study of the solutions regarding the influence of geometry on the structure's stress is based on the following main directions:

- dimensioning of the shell of the board in the affected area for increasing the resistance at impact (variant II,  $E=100$  kJ,  $v=10$  m/s);
- dimensioning of the frame of the affected area to diminish the effects of the impact (variant I,  $E=400$  kJ,  $v=20$  m/s);
- dimensioning of the border of the affected area to increase the resistance at impact and diminish its effects (variant II,  $E=400$  kJ,  $v=20$  m/s).
- modification of the frame's curvature to diminish the effects of the impact (variant III,  $E=100$  kJ,  $v=10$  m/s).

4) Modification of the structure's geometry of the barge's bow, whose main objectives are to reduce the structure's stress and the damaged area as a result of the impact. Development of six 3D FEM structural models for compared analyses. The following gains are obtained:

- the structure's Von Mises stresses reduction of 3.47% compared to the similar values of the initial geometry, for the variant in which the energies generated the plastic stage, by dimensioning the geometrical characteristics of the structure (variant I,  $E=100$  kJ,  $v=10$  m/s);
- canceling the effects of the impact in the damaged area on the boarding, for the variants in which the energies generated the plastic stage, by dimensioning the geometrical characteristics of the structure (variant II,  $E=100$  kJ,  $v=10$  m/s);
- 29.65% reduction of the area and 1.67% of the volume of the damaged structure, for the variants in which the energies generated the rupture stage compared to similar values of the initial geometry, by dimensioning the geometrical characteristics of the structure (variant I,  $E=400$  kJ,  $v=20$  m/s);
- 11.54% decrease of the damaged area on the board only for  $\mu = 0.0$ , compared to initial structure, by modifying the curvature of the frame, which allows an increase in the buoyancy of the new geometry (variant III,  $E=400$  kJ,  $v=20$  m/s).

5) Development of the design methodology for the construction of a structure that will provide an appropriate behavior at impact.

6) Development a fast methodology for calculating impact situations where damage occurs that can cause flooding of compartments or even sinking the ship so that decisions can be made to solve problems effectively

### 6.3. Future research perspectives

1) A broader approach to the behavior of the ship structure in the plastic field, using a coupled method that consider simultaneously the hydrodynamic behavior of the model, which also includes inertia forces, global, local and impact demands.

2) Carrying out experiments as much as possible on structures on a natural scale (something that at the moment has been done by very few researchers due to the costs involved), for studying the influence of friction and various materials, allowing to expand the calculation methods for material yielding.

3) The solutions investigated in this paper can be used to optimize the procedures related to the repair of damaged barges.



4) In view of the concern for the protection of the environment, regarding the traffic on inland waters, it becomes necessary that in the future this type of analysis be included as a design rule of classification societies, for all categories of ships. The rules could target:

- achievement of risk curves at impact, by determining the stresses under impact loads, along the length of the ship;
- more precise determination of critical plastic deformations, rupture, etc.



**BIBLIOGRAPHY**

- [ 1 ] Domnişoru L, *Analiza structurală și hidroelasticitatea navelor*, Galați, Editura Fundației Universitare "Dunărea de Jos" Galați, 2006, pag.300-350;
- [ 2 ] Petersen M.J. , *Dynamics of Ship Collision*, Ocean Engineering, Vol.9, No.4, pag. 295-329, 1982;
- [ 3 ] Woisin G., *Instantaneous loss of energy with unsymmetrical ship collision*, Schiff&Hafen, Vol.40, No.1, pag.50-55,1988;
- [ 4 ] Pawlowski M., *Energy loss in ship's collisions*, Centrum Techniki Okretowej, Poland, 1995;
- [ 5 ] Hanhirova H., *External collision model, safety of passanger/RoRo Vessels*, Helsinki ,University of Technology, Ship Laboratory, Oct.1995;
- [ 6 ] Zhang S., *The mechanics of ship collision*, Technical University of Denmark, Denmark
- [ 7 ] Minorsky V.U., *An analysis of ship collision with reference to protection of nuclear power ships* , J. of Ship Research, Vol. 3, No.2, pag.1-4, 1959;
- [ 8 ] Woisin G., *Design against collision*, Schiff&Hafen, Vol.31, No.2,pag. 1059-1069, Germania, 1979;
- [ 9 ] Vaughan H., *Bending and tearing of plate with application to ship bottom damage*, Naval Architects, Vol. 3, pag.97-99, 1978;
- [10] Reckling K.A., *Mechanism of minor ship collision*, Int.J. of Impact Engineering, Vol.13, No.2, pag.163-187,1983;
- [11] Pedersen P.T., Valsgaard S., Olsen D., Spangenberg S.I., *Ship impact: Bow collisions*, Int.J. of Impact Engineering, Vol.13, No.2, pag.163-187,1993;
- [12] Gerard G., *The crippling strength of compression element*, Int.J. of Aeronautical Science, 1958;
- [13] Amdahl J., *Energy absorption in ship-platform impact*, Norwegian Institute of Technology, Report No.UR-83-34, 1983;
- [14] Yang P.D.C. și Caldwell J.B., *Collision energy absorption of ship bow structure*, Int. J. Impact Engineering, Vol.b 7, No. 2, pp. 181-196,1988;
- [15] Pedersen P.T., *Ship crushing load studies*, Chapter 3.6, East Bridge, The Storebelt Publications, Editor Niels Gimsing, pag.44-57,1998;
- [16] Wierzbicki T., Abramowicz W., *On the crushing mechanism of thin walled structures*, Journal of Applied Mechanism, Vol. 50, 1983;
- [17] Wierzbicki T., Thomas P., *Closed-form solution for wedge cutting force through thin metal sheet*, Int. J. Mech. Sci, Vol.35, No. 3/4, pag. 209-229, 1993;
- [18] Abramowicz W., *Crushing resistance of T.Y. and X section*, MIT-Industry joint program on tanker safety, Massachusetts Institute of Technology, U.S.A., Report No. 24, 1994;
- [19] Kierkegaard H. , *Ship bow response in high energy collision*, Marine Structure, No.6, 1993;
- [20] Paik J.K., Pedersen P.T., *Ultimate and crushing strength of plated structures*, J. of ship research, Vol.39, No.3, pag.340-348, 1995;
- [21] Simonsen B.C., *The mechanism of ship grounding*, Technical University of Denmark, Ph.D.thesis, 1997;
- [22] Jones N., *Structural impact*, Cambridge University Press, 1989;
- [23] Jones N.,Wierzbicki T., *Structural crashworthiness and failure*, Elsevier Applied Science, 1993;
- [24] Wang G., *Structural analysis of ship collision and grounding*, Ph.D.thesis, University of Tokyo, 1995;
- [25] Wen H.M, Jones M., *Experimental investigation of the scaling laws for metals plates struck by large masses*, Int. J.Impact Engineering, vol. 13, no. 3, pag. 485-505,1993;

- [26] Amdahl J. și Kavlie D. , *Experimental and numerical simulation of double hull standing*, DNV-MIT Work Shop on Mechanism of Ship Grounding, DNV, Norway, 1992;
- [27] Amandl J., *Side collision*, 22<sup>nd</sup> WEGEMENT Graduate School, Technical University of Denmark, 1995;
- [28] McDermott J., Kline R., Jones E., Maniar N. and Chiang W., *Tanker structural analysis for minor collision*, SNAME Transactions, 1974;
- [29] Jones N., *A Literature survey on the collision and grounding protection of ships*, Ship Structurers Committee Report, SSC-283,1979;
- [30] Ellinas E.D. și Valsgard S., *Collision and damage of offshore structures a state of art*, 4th Int. Symposium on Offshore Mechanics and Arctic Engineering, Dallas, Texas, February 17-22, 1985;
- [31] Samuelides E și Frieze P.A., *Fluid structure interaction in ship collision*, Marine Structures, Vol.2.,pp.65-88,1989.
- [32] Akita Y., s.a., *Studies on collision-protective structures in nuclear powered ships*, Nuclear Engineering Design, No.19, 1972;
- [33] Ito H. s.a., *A simplified method to analysis the strength of double hulled structures in collision*, 1<sup>st</sup> report, J. of Naval Arch. Of Japan, 1984;
- [34] Qvist S. s.a., *Ship Collision . Experimental and numerical analysis of double hull models*, 9<sup>th</sup> DYMAT Technical Conference,1995;
- [35] Hagiwara K., Takanabe H., Kawano H., *A proposed method of predicting ship collision damage*, Int.J. of Impact Engineering, Vol.I, No.3,1983;
- [36] Abramowicz W. și Jones N., *Dynamic progressive buckling of circular and square tubes*, Int.J. of Impact Engineering, Vol. 4, No. 4, pp.243-270, 1986;
- [37] Ishiyama S., s.a. , *Impact response of thin walled plane frame structures*, Int. J. Impact. Eng, Vol. 1, No.3, pag.227-247, 1983;
- [38] Simonsen B.C. și Ocakli H., *Experiments and theory on deck and girder*, 1999;
- [39] Kitamura O., *Comparative study on collision resistance of side structure*, International Conference on Design and Methodologies for Collision and Grounding Protection of Ships, San Francisco, California, U.S.A. August 22-23, 1996, " Marine Technology", Vol. 34, No.4, pag.293-308, 1997;
- [40] Sano A., Muragish O. și Yoshikawa T., *Strength analysis of a new double hull structure for VLCC in collision*, International Conference on Design and Methodologies for Collision and Grounding Protection of Ships, San Francisco, California, U.S.A, August, 22-23, 1996;
- [41] Kuroiwa T., *Numerical simulation of actual collision & grounding accidents*, International Conference on Design and Methodologies for Collision and Grounding Protection of Ships, San Francisco, California, U.S.A., August 22-23, 1996;
- [42] Cook R.D., Malkus D.S., Plesha M.E., Witt R.H., *Concepts and application of finite element analysis*, 2002;
- [43] Myhre S.A., *Analysis of accidental iceberg impacts with membrane tank LNG carriers - Master Thesis*, Norwegian University of Science and Technology, Norway, 2010;
- [44] Ansys Inc., *ANSYS Release 13.0 Guide*, Ansys Inc., USA, 2010;
- [45] Livermore Software Technology Corporation (LTSC) : *LS-DYNA*, Livermore, California, USA, [www.ltsc.com/products/ls-dyna](http://www.ltsc.com/products/ls-dyna);
- [46] Bălan M., Domnișoru L., *Numerical analysis of a ship side collision structural response based on the finite element method*, Annals of "Dunarea de Jos" University of Galati, Galati University Press, pag. 51-60, 2012;
- [47] Bathe, K.J., Chapelle, D., *The Finite Element Analysis of Shells. Fundamentals*, Springer Publishing House, 2nd ed, 2011;

- [48] Liu Z., Amdahl J. " A new formulation of the impact mechanics of ship collision and its application to a ship-iceberg collision", *Marine Structure*, Elsevier Press, pag.360-384, 2010;
- [49] Pedersen, P.T., Li, Y., *On the global ship hull bending energy in ship collision*, *Marine Structures*, Vol. 22, No 1, pag. 2-11, Elsevier LTD, England, DOI://org.doi/10.1015/marstruc.2008.06.005, 2009;
- [50] Gom mbH, Calibration, *Aramis User Manual -Software*, pag. 4-7, 2007;
- [51] \*\*\*, <http://www.dnvgl.com>, *DNVGL-RP-C204 Recommended practice – Design against accidental loads*, 2017;
- [52] \*\*\*, Autoritatea Navală Română- *Albumul tipurilor de nave*, 2006;
- [53] Domnisoru, L, *Special chapters on ship's structures analysis. Applications*. Editura Fundației Universitare 'Dunărea de Jos' Galați, ISBN 978-973-627-589-0, 2017;
- [54] Liu C.Y., Glass D., *Effects of mesh density on finite elements analysis*, SAE World Congress & Exhibition, <https://doi.org/10.4272/2013-01-1375>, 2013;
- [55] \*\*\*, <http://www.dnvgl.com>, *DNVGL-CG-0127 Class guideline – Finite element analysis*, 2018;
- [56] Alsos S. H., Amdahl J., *On the resistance to penetration of stiffened plates, Part 1- Experiments*, *Int. J. Impact Eng.*, Vol. 36, pag. 799- 807, 2009;
- [57] \*\*\*, <http://www.dnvgl.com>, *DNV-GL-RP- C208 Recommended practice - Determination of structural capacity by non-linear finite element analysis methods*, 2013;
- [58] \*\*\*, <http://www.dnvgl.com>, *DNV GL-OS-C102- Structural design of offshore ships* , 2018;
- [59] Orymowska J., Sobkowicz P., *Navigational safety of inland vessels in the Międzyodrze and Szczeciński Węzeł Wodny area*, *Scientific J. of the Maritime Univ. of Szczecin*, Vol. 49, pag. 93-99, 2017;
- [60] Guerro D., *Impact of transport connections on port hinterlands*, *Regional Studies*, Vol. 53, No. 4, pag. 540- 549, 2019;
- [61] Popa C, Barbu G, *Managementul transporturilor pe apele interioare*. Editura Constanța, 2013;
- [62] Sha, YY., Amandl, J., Liu, K., *Design of steel girder against ship forecastle*, *Engineering Structures*, Vol. 196, Elsevier SCI LTD, England, DOI: 10.1016/j.engstruct.2019.109277, 2019;
- [63] Fan, W., Yuan, WC., *Ship bow force-deformation curves for ship impact demand of bridges considering effect of pile-cap depth*, *Shock and Vibration*, Hindawi Publishing Corporation, USA, DOI: 10.1155/2014/201425, 2014
- [64] Wang L, Yang L., Huang D., Zhang Z., Chen G., *An aspect of a dynamic analysis on a new crashworthy device against ship-bridge collision*, *Int. J. Impact Eng.*, Vol. 35, pag.895-904. 2008;
- [65] \*\*\*, <http://www.femap.com>, *Femap User Guide version 11.3*, Siemens Product Lifecycle Management Software, 2016;
- [66] \*\*\*, *NX Nastran Getting Started Tutorials*, Siemens Product Lifecycle Management Software, 2014;
- [67] \*\*\*, *NX Nastran - Theoretical Manual* , Siemens Product Lifecycle Management Software, 2014.